

RATE TRANSIENT ANALYSIS AND COMPLETION OPTIMIZATION STUDY IN EAGLE
FORD SHALE

By

Chaitanya Borade

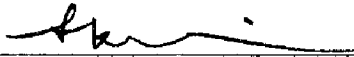
RECOMMENDED:



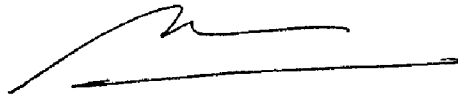
Dr. Shirish Patil
Advisory Committee Chair



Abhijeet Inamdar
Advisory Committee Member



Dr. Sanatanu Khataniar
Advisory Committee Member



Dr. Abhijit Dandekar,
Advisory Committee Member
Chair, Department of Petroleum Engineering

8/10/2015

Date

RATE TRANSIENT ANALYSIS AND COMPLETION OPTIMIZATION STUDY IN EAGLE
FORD SHALE

By
Chaitanya Borade

RECOMMENDED:

Dr. Shirish Patil
Advisory Committee Chair

Abhijeet Inamdar
Advisory Committee Member

Dr. Sanatanu Khataniar
Advisory Committee Member

Dr. Abhijit Dandekar,
Advisory Committee Member
Chair, Department of Petroleum Engineering

Date

RATE TRANSIENT ANALYSIS AND COMPLETION OPTIMIZATION STUDY IN EAGLE
FORD SHALE

A
MASTER'S PROJECT

Presented to the Faculty
of the University of Alaska Fairbanks

In Partial Fulfillment of the Requirements
for the Degree of

MASTER OF SCIENCE

Chaitanya Borade, B.Sc

Fairbanks, AK

August 2015

Abstract

Analysis of well performance data can deliver decision-making solutions regarding field development, production optimization, and reserves evaluation. Well performance analysis involves the study of the measured response of a system, the reservoir in our case, in the form of production rates and flowing pressures. The Eagle Ford shale in South Texas is one of the most prolific shale plays in the United States. However, the ultra-low permeability of the shale combined with its limited production history makes predicting ultimate recovery very difficult, especially in the early life of a well. Use of Rate Transient Analysis makes the analysis of early production data possible, which involves solving an inverse problem. Unlike the traditional decline analysis, Rate Transient Analysis requires measured production rates and flowing pressures, which were provided by an operator based in the Eagle Ford.

This study is divided into two objectives. The first objective is to analyze well performance data from Eagle Ford shale gas wells provided by an operator. This analysis adopts the use of probabilistic rate transient analysis to help quantify uncertainty. With this approach, it is possible to systematically investigate the allowable parameter space based on acceptable ranges of inputs such as fracture length, matrix permeability, conductivity and well spacing. Since well spacing and reservoir boundaries were unknown, a base case with a reservoir width of 1500 feet was assumed. This analysis presents a workflow that integrates probabilistic and analytical modeling for shale gas wells in an unconventional reservoir. To validate the results between probabilistic and analytical modeling, a percent difference of less than 15% was assumed as an acceptable range for the ultimate recoverable forecasts.

Understanding the effect of existing completion on the cumulative production is of great value to operators. This information helps them plan and optimize future completion designs while reducing operational costs. This study addresses the secondary objective by generating an Artificial Neural Network model. Using database from existing wells, a neural network model was successfully generated and completion effectiveness and optimization analysis was conducted. A good agreement between the predicted model output values and actual values ($R^2 = 0.99$) validated the applicability of this model. A completion optimization study showed that wells drilled in condensate-rich zones required higher proppant and liquid volumes, whereas wells in gas-rich zones required closer cluster spacing. Analysis results helped to identify wells which were either under-stimulated or over-stimulated and appropriate recommendations were made.

Acknowledgements

I would like to express my sincere thanks to my principal advisor, Dr. Shirish Patil for his invaluable guidance and support during my graduate studies. I also greatly appreciate my advisory committee members Dr. Abhijit Dandekar, Dr. Santanu Khataniar and Abhijeet Inamdar for their valuable suggestions and commitment to this project. I would also like to extend my thanks to Amir Pashahang and Lisset Sousa at Statoil for their feedback during my project.

This project wouldn't have been possible without the donation from IHS-Fekete. I want to thank them for their technical support during my project work.

I express my deepest gratitude to my parents, Mr. Sunil and Mrs. Shobhana Borade, for their unconditional love and support. Finally, I would like to thank my faculty and friends for their support during my time at UAF.

Table of Contents

Abstract.....	3
Acknowledgements.....	4
CHAPTER 1 Introduction.....	10
1.1 Unconventional Resources.....	10
1.2 Shale Resources	11
1.3 Shale Resources in Texas.....	13
1.4 Objective for Studying Eagle Ford	14
CHAPTER 2 Literature Review.....	15
2.1 Eagle Ford Shale	15
2.1.1 Eagle Ford Shale Geology	15
2.2 Introduction to Hydraulic Fracturing	18
2.3 Hydraulic Fracturing Theory	21
2.3.1 Multi-stage Hydraulic Fracturing.....	21
2.3.2 Completion Techniques	22
2.3.3 Fracturing Fluid Selection.....	24
2.3.4 Proppant Selection and Availability.....	24
2.3.5 Fracture Conductivity	25
2.3.6 Methodology to Select Optimum Hydraulic Fracture Design.	25
CHAPTER 3 Traditional vs. Modern Decline Analysis	26
3.1 Part 1 - Uncertainty in Production Data Analysis.....	27
3.2 Pre-analysis Diagnostics	29
3.3 Flow Regimes	30
3.4 Flowing Material Balance Analysis Theory	34
3.4.1 Pseudo-Steady State.....	34
3.5 Analytic Model – The Enhanced Fracture Region Deterministic Model.....	36
3.6 Uncertainty Modeling & Modified Workflow	38
3.7 Procedure	40
3.8 Base Case: Reservoir Width = 1500 ft.....	40
3.9 Data Analysis & Results	45
3.10 Deterministic & Probabilistic Results.....	46
CHAPTER 4 Part 2 - Completion Effectiveness & Performance Drivers	50

4.1	Artificial Neural Network	52
4.1.1	Parameter Selection for Modeling	53
4.2	Artificial Neural Network Generated – 5 Month Production Model	54
4.3	Parameter Sensitivity	55
4.4	Completion Optimization.....	59
CHAPTER 5	Conclusions and Recommendations	63
CHAPTER 6	Appendix.....	65
CHAPTER 7	Nomenclature	69
CHAPTER 8	References.....	70

List of Figures

Figure 1.1 Hydrocarbon Resource Triangle 10

Figure 1.2 U.S. tight oil and gas production from different shale plays across nation 12

Figure 1.3 Lower 48 Shale plays 13

Figure 2.1 Color coded map of Eagle Ford Shale Play in South Texas 15

Figure 2.2 Eagle Ford Shale Structure Map 16

Figure 2.3 Eagle Ford Productive Oil and Gas Wells in their representative windows 17

Figure 2.4 Eagle Ford type logs highlighting the stratigraphic differences across the area, La Salle & Karnes County 18

Figure 2.5 A typical Hydraulic Fracturing job 19

Figure 2.6 Hydraulic Fracturing Treatment plot 19

Figure 2.7 Natural Completion vs. Hydraulic Fracture Completion (Bukola & Aguilera, 2014). 20

Figure 2.8 Horizontal Well with Multi-Stage Fracture Technology 20

Figure 2.9 Components of Hydraulic Fracturing Models 21

Figure 2.10 Example of multi-stage hydraulic fracturing operation. Halliburton’s Swell packer system isolating various zones of a horizontal wellbore that will be stimulated. 22

Figure 2.11 Plug-and-Perf Completion System 23

Figure 2.12 Ball activated Completion System 23

Figure 2.13 Coil Tubing –Activated Completion System 23

Figure 2.14 Methodology for selecting optimum fracturing design 25

Figure 3.1 Recommended Approach in terms of Modern Production Analysis 27

Figure 3.2 Rate Transient Analysis Workflow 29

Figure 3.3 Enhanced Fracture Region Model with associated well performance profile 32

Figure 3.4 Tri-Linear Flow Model (left) vs. Enhanced Fracture Region Model 33

Figure 3.5 Square Root Time plot analysis passing through origin and negative intercept (Fekete Associates Inc.) 33

Figure 3.6 Pseudo-steady state conditions for a given well 35

Figure 3.7 Flowing Material Balance Plot 36

Figure 3.8 Horizontal well with multiple branch fractures (left) and its representative model (right), $k_1 > k_2$ 37

Figure 3.9 Enhanced Fracture Region Model Schematic 37

Figure 3.10 Schematics & Dimensions for five-region model 38

Figure 3.11 IHS-RTA software schematic for initialization data 40

Figure 3.12 Square Root Time plot in the Unconventional Model 43

Figure 3.13 Schematic for the Most-Likely Approach 43

Figure 3.14 Modified Workflow adopted for this analysis 44

Figure 3.15 Fracture half-length values for each well using both approaches. 48

Figure 3.16 Bar chart for matrix permeability for both approaches 48

Figure 3.17 Deterministic vs. Probabilistic Approach EUR output 49

Figure 4.1 Plots for Total Gp vs. Design Parameters 50

Figure 4.2 Comparison plots for 5 month cumulative production to different design parameters	51
Figure 4.3 Single input neuron process	52
Figure 4.4 Initial condensate gas ratio for each well	54
Figure 4.5 ANN Model Regression Plot.....	55
Figure 4.6 ANN Model Predicted vs. Actual Values	55
Figure 4.7 Bar Chart for 5 Month Production Model – Parameter Sensitivity Completion Effectiveness	56
Figure 4.8 Bar chart for change in cluster spacing by 50%.....	57
Figure 4.9 Bar chart for amount of Proppant pumped by 50%.....	57
Figure 4.10 Bar Chart for change in number of stages.....	58
Figure 4.11 Bar chart for change in amount of Liquid Pumped.....	58
Figure 4.12 Bar Chart for Well C-2 Completion Scenarios Results.....	61
Figure 4.13 Bar Chart for Well K Completion Scenarios.....	62
Figure 6.1 Flow directions & boundary conditions for Five-Region Model	65

List of Tables

Table 1.1 Top 10 countries with technically recoverable shale oil resources.	11
Table 1.2 Top 10 countries with technically recoverable shale gas resources.	12
Table 3.1 Parameter and their respective constraints within the EFR analytical model	42
Table 3.2 Uncertainty Distribution for each parameter within probabilistic modeling.....	42
Table 3.3 List of provided wells for analysis. Only gas wells were analyzed (in blue)	45
Table 3.4 Deterministic Results for all wells.....	47
Table 3.5 Probabilistic Results for all wells	47
Table 4.1 Input Parameter for ANN modeling summary	54
Table 4.2 Summary of all the varied parameters for each well	59
Table 4.3 Scenario Results Summary for Well C-2.....	61
Table 4.4 Scenario Results for Well K	62

CHAPTER 1 Introduction

This section briefly introduces the presence of shale reservoirs under unconventional resources with an emphasis on the status and its future potential. This information is followed by the recent practices for developing shale resources.

1.1 Unconventional Resources

The shift from conventional resources to unconventional resources is the result of an exponential increase in global energy consumption. Conventional resources can be defined as formations where production is economically viable without requiring any specialized techniques. Unconventional resources can be defined as hydrocarbon reservoirs with low permeability and cannot produce economical volumes without the application of stimulation processes such as fracturing. Coalbed methane, Methane Gas Hydrates, shale gas, tight gas, oil shale, and heavy-oil are all forms of unconventional energy resources.

Masters and Gray (1979) published the concept of the resource triangle, showing that all-natural resources are log-normally distributed in nature. The resource triangle (Figure 1.1) shows that the high-grade deposits, which are difficult to find but easy to extract, lie in the top of the triangle and are small in size. The reservoir quality declines as we descend the triangle; unconventional resources form the base. Adequate product price and improved technology are required to exploit these resources. However, the deposit size of unconventional resources is larger than that of high-quality conventional resources (Holditch, 2009).

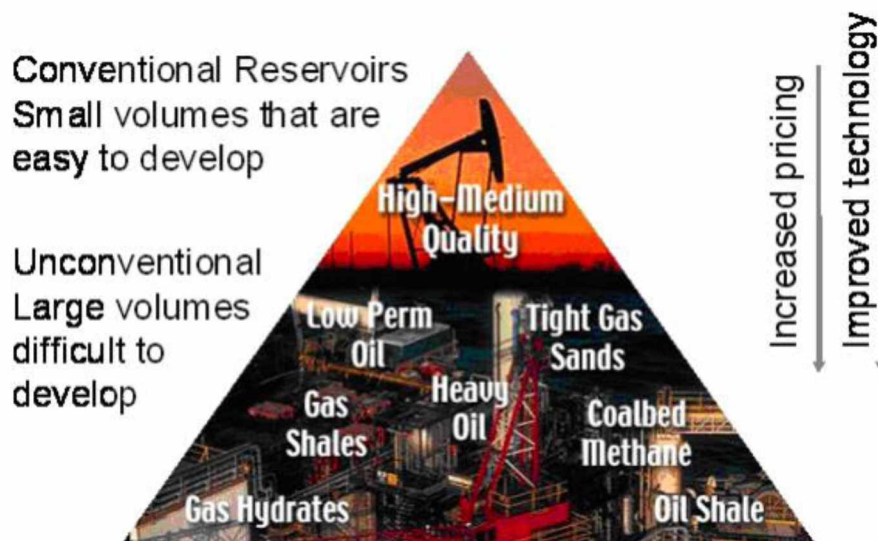


Figure 1.1 Hydrocarbon Resource Triangle (Holditch, 2009).

1.2 Shale Resources

A strict geological definition of shale is any “laminated, indurated (consolidated) rock with > 67% clay-sized materials” (Jackson, 1997). Shale formations are often deposited in low-energy environments, high in organic content, fine-grained, and low-permeability. They are usually considered potential source and/or seal rocks for conventional hydrocarbon reservoirs. Recent developments in horizontal drilling and hydraulic fracturing have made commercial oil and gas production from low permeability shale formations possible. Such advancements have made it possible to consider shale formations as potential unconventional hydrocarbon reservoirs, although with significant lower permeability than conventional resources.

The Annual Energy Outlook presented by the U.S. Energy Information Administration reports technically recoverable resources of 345 billion barrels of world shale oil and 7299 trillion cubic feet of world shale gas. Technically recoverable resources can be used interchangeably with economically recoverable resources, hence, it is necessary to distinguish them. Under current market conditions, economically recoverable resources are those which can be profitably produced, whereas technically recoverable resources are producible volumes of oil and gas with the current technology regardless of the current market. The U.S. is at the forefront in developing shale plays and ranks among the top 10 countries with technically recoverable shale oil and gas resources (Table 1.1 & 1.2).

Table 1.1 Top 10 countries with technically recoverable shale oil resources (EIA, 2014).

Rank	Country	Shale oil (billion barrels)	
1	Russia	75	
2	U.S. ¹	58	(48)
3	China	32	
4	Argentina	27	
5	Libya	26	
6	Australia	18	
7	Venezuela	13	
8	Mexico	13	
9	Pakistan	9	
10	Canada	9	
World Total		345	(335)

¹ EIA estimates used for ranking order. ARI estimates in parentheses.

Table 1.2 Top 10 countries with technically recoverable shale gas resources (EIA, 2014).

Rank	Country	Shale gas (trillion cubic feet)	
1	China	1,115	
2	Argentina	802	
3	Algeria	707	
4	U.S. ¹	665	(1,161)
5	Canada	573	
6	Mexico	545	
7	Australia	437	
8	South Africa	390	
9	Russia	285	
10	Brazil	245	
World Total		7,299	(7,795)

¹ EIA estimates used for ranking order. ARI estimates in parentheses.

Tight oil and shale gas resources have revolutionized U.S. oil and natural gas production, providing 29% of total U.S. crude oil production and 40% of total U.S. natural gas production in 2012 (EIA Annual Energy Outlook 2013). This domestic increase can be attributed to the continuous growth in hydrocarbon production from shale formations across the nation. Production from shale plays has increased significantly from 2007 onwards, as shown in Figure 1.2, and will increase with the given forecast and developments in technology.

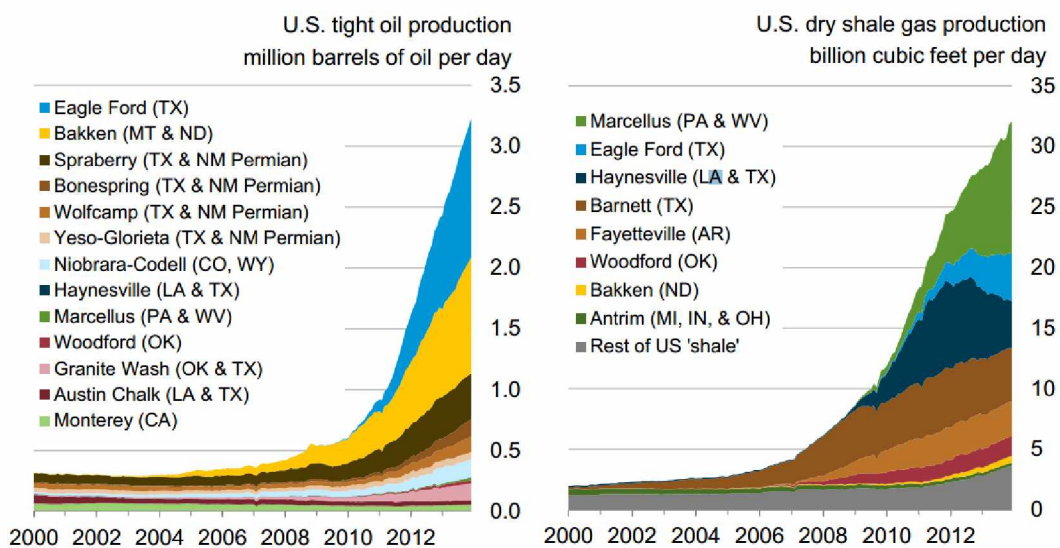


Figure 1.2 U.S. tight oil and gas production from different shale plays across the nation. (EIA 2014)

1.3 Shale Resources in Texas

Fracturing techniques saw a growth in application since the early 1950s but were not deployed in the fields of Texas until the 1980s. The introduction of directional drilling and the advent of improved downhole drilling supported fracturing in shale reservoirs. Mitchell Energy Corporation was the first oil and gas company to unsuccessfully try the foam fracturing (frac) method in the Barnett Shale of North-Central Texas. Due to uneconomic results using this method, Mitchell Energy adopted the nitrogen gel-water frac, which yielded economical production. Recognizing this commercial success in unconventional reservoirs, several companies aggressively entered this play, and by 2005 the Barnett Shale alone was producing nearly 0.5 trillion cubic feet (EIA, 2011). Combined with the development in horizontal drilling, several shale plays were successfully targeted, boosting an economic confidence and technological development in the industry. Figure 1.3 shows several current and prospective shale gas and shale oil plays across the U.S. The Barnett Shale and the Eagle Ford formations make up most of the Texas shale plays.

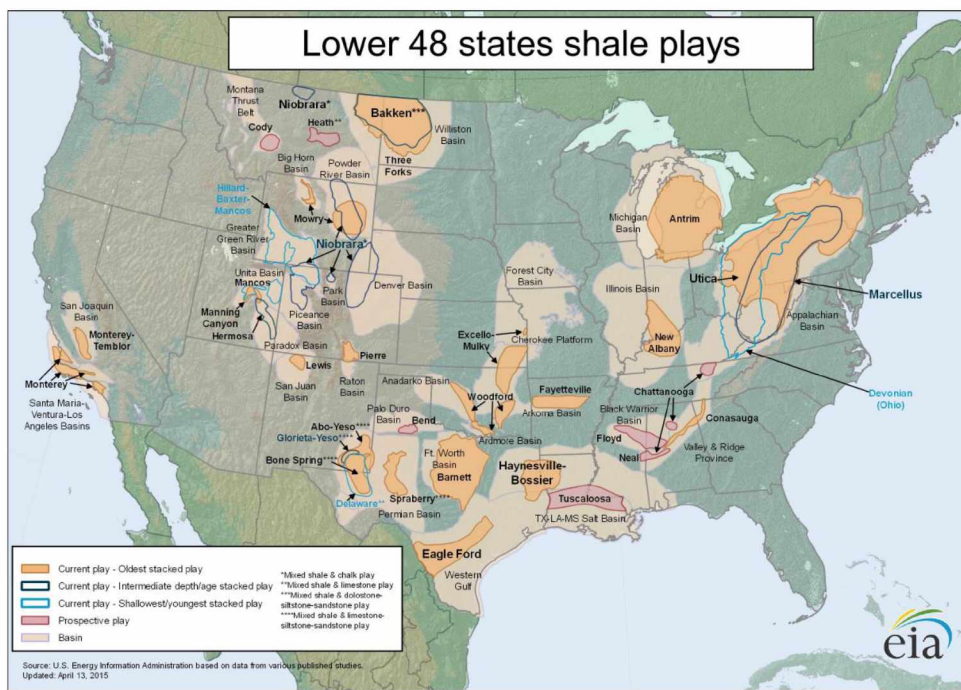


Figure 1.3 Lower 48 Shale plays. (EIA 2015, http://www.eia.gov/oil_gas/rpd/shale_gas)

1.4 Objective for Studying Eagle Ford

Recent advances in horizontal drilling have allowed exploiting unconventional resources at lower costs. Several major oil and gas are operating in the Eagle Ford shale and an assessment of the oil and gas resources and the associated uncertainty in the early stage is critical for future developments. But due to the complexity of the well and the reservoir system it is a difficult task to evaluate the well potential and interpret an appropriate reservoir description. The main objective of this analysis is to evaluate well performance from wells located in Eagle Ford and interpret the well potential in terms of Estimated Ultimate Recovery (EUR). The secondary objective of this project is to evaluate the existing well-completions and verify if the potential for completion optimization through different completion and fracturing scenarios. This information is of great value to E&P companies in regards to further their knowledge in accessing existing reservoir assets and use it for future developments.

CHAPTER 2 Literature Review

2.1 Eagle Ford Shale

Located in the Western Gulf Basin, the Eagle Ford shale formation has produced more oil than any other traditional shale play. This shale play began with the horizontal discovery well STS #1 in October 2008 (initial production 9.7 Mcf/d from a 3200 ft. lateral). Since its initial discovery, the shale play has expanded from the discovery well in La Salle County, Texas to the Mexican border and northeast to the eastern border of Gonzales and Lavaca Counties (Martin et al., 2011). The Sligo shelf edge is widest, extending northward to encompass the Maverick basin and almost parallel to the southern border. The area of the trend is 102 miles long by an average of 60 miles wide (Martin et al., 2011). The Eagle Ford shale play is divided into oil, wet gas/condensate, and dry gas windows. Figure 1.4 shows a color-coded map of the Eagle Ford Shale play in the Western Gulf Basin of South Texas.

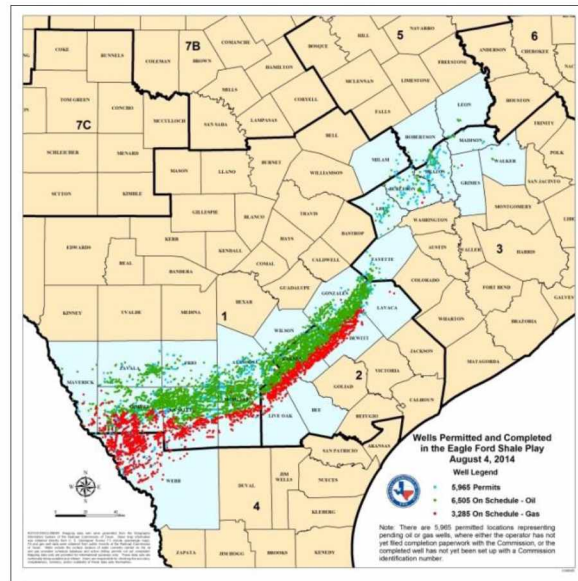


Figure 2.1 Color-coded map of Eagle Ford Shale Play in South Texas (RRC 2014, <http://www.rrc.state.tx.us/oil-gas/major-oil-gas-formations/eagle-ford-shale/>).

2.1.1 Eagle Ford Shale Geology

Traditionally known as the source rock for the Austin Chalk oil and gas formation, the Eagle Ford Shale is a Late Cretaceous (Cenomanian – Turonian) formation. The shale content increases towards Webb County in the southwest, while the carbonate shale percentage increases up to 70% in the northeast. The higher carbonate content and lower clay content make the Eagle Ford shale more brittle, thus more favorable for fracking. Figure 1.5 shows a structure map of the Eagle Ford Shale with the outcrop in black

and the rock unit dipping towards the southeast as it approaches Gulf of Mexico. The productive areas of the Eagle Ford were deposited in a low-energy marine environment, believed to be deep and far enough from shore to avoid wave disturbance. Its rich organic content gives the shale a dark color. The anoxic waters during deposition helped protect the organic material from decay and the laminations from bioturbation. The upper Eagle Ford transgressive facies contains thinly bedded limestones, shales, siltstones, and bentonites with an overlying regressive condensed section unit. The formation contains very little quartz and feldspar. It has an average total organic carbon (TOC) of 2.45 wt. % +/- 1.49% and kerogen type varies from II-IV in Brazos and Burleson counties, Texas (Sondhi, 2011).

The Eagle Ford Shale averages 250 ft across the play but can reach up to 400 ft in thickness. The burial depths during deposition dictate where oil and gas are located within the formation. Due to sufficient exposure to heat and pressure, organic material converted to oil is found around depths of 4000 ft and natural gas is formed at greater depths. The Eagle Ford Shale is not characterized by natural fractures but is well known for producing variable amounts of dry gas, wet gas, NGLs, condensate, and oil. Figure 2.3 shows the geographic distribution of the oil and natural gas production windows in the Eagle Ford Shale.

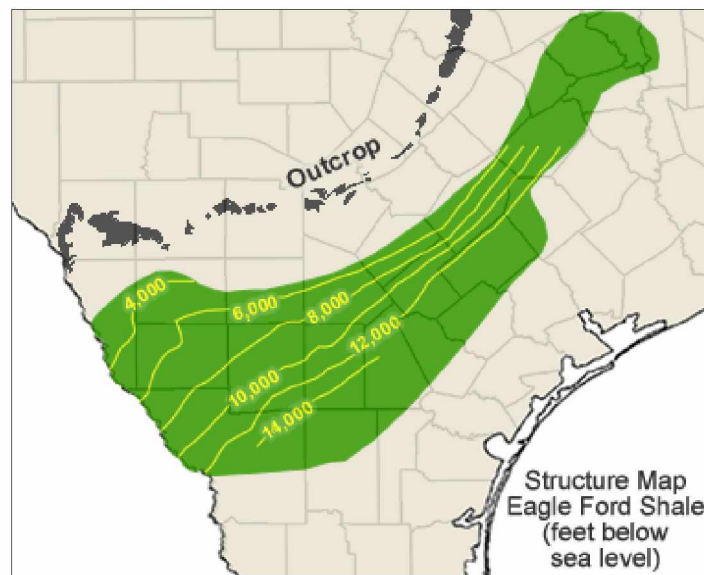


Figure 2.2 Eagle Ford Shale Structure Map. (<http://geology.com/articles/eagle-ford/>)

The green areas are where the production activity is limited to natural gas, the red areas are limited to oil wells, and the yellow area typically yield both oil and gas wells. This information agrees with the Eagle Ford Shale structure map (Fig. 2.2).

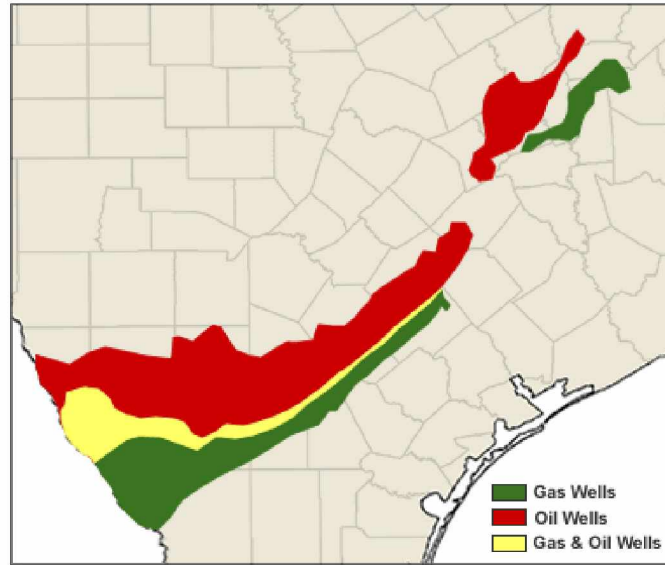


Figure 2.3 Eagle Ford Productive Oil and Gas Wells in their representative windows (<http://geology.com/articles/eagle-ford/>).

The Eagle Ford is broken down into two intervals for classification purposes. The lower section of Eagle Ford consists of a transgressive marine interval dominated by dark, laminated, organically rich shale, while the regressive section consists of interstratified calcareous shales, bentonites, limestones, and quartzose siltstones (Martin et al., 2011). The second log in Figure 2.4 highlights both the transgressive shales and the regressive intervals, which are located in the Karnes County. Reservoir properties vary across the entire area of Eagle Ford, with key properties such as effective porosity ranging between 3% and 10% with a mean of 6%, and matrix permeability ranging between 3 nD and 405 nD, with an average of 180 nD.

The transgressive interval is primarily the organic-rich shale deposited by shallow warm seas, whereas the upper regressive interval is a transition to a near-shore environment (Martin et al., 2011). The southwest depositional area is quite different from the northeast area, since it is characterized as a restricted basin bounded by the Edwards shelf edge to the north and the shoreline to the south. This characterized the regressive upper Eagle Ford Shale as black shale due to its prevalence in oxygen-poor environment (Dawson, 2000). Due to its depositional environment, the Eagle Ford Shale is considered one of many world-class source rocks. But due the ultra –low matrix permeability characteristics of Eagle Ford shale, hydraulic fracturing stimulation is the only method from which economical production would be possible. A detail discussion of this method is presented in the following section.

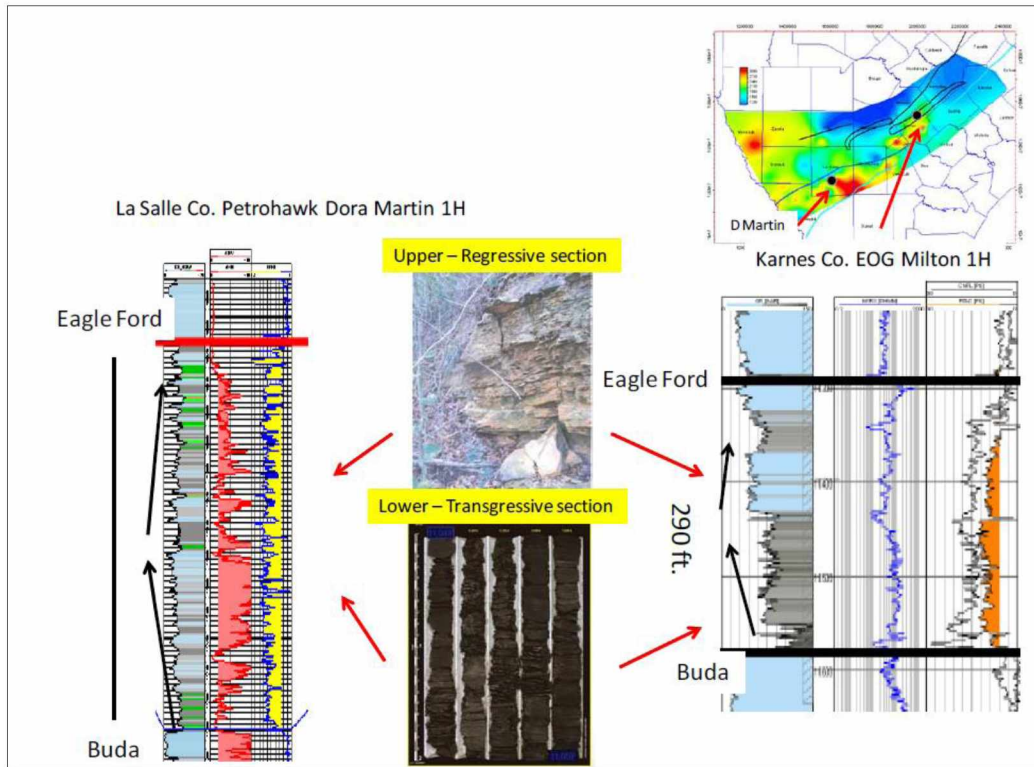


Figure 2.4 Eagle Ford type logs highlighting the stratigraphic differences across the area, La Salle & Karnes. County (Martin et al., 2011).

2.2 Introduction to Hydraulic Fracturing

Hydraulic fracturing is a physical process in which specially engineered fluids are pumped into the formation at high rates and pressures to increase the fluid pressure above the minimum stress in order to initiate a fracture. This provides a conductive path from the reservoir to the wellbore by enhancing the reservoir permeability through increasing the area of contact due to fracture propagation. The first attempt at hydraulically fracturing a formation was made by Halliburton and Stanolind Oil in 1947 in the Hugoton gas field, Grant County, southwestern Kansas. Since its commencement, hydraulic fracturing has seen extreme technological advancements, which have led to its wide use in the stimulation process.

A conventional fracturing process consists of three stages, as shown in Figure 2.5. To create a fracture, a fluid stage known as pad is pumped first at high injection rates. This stage is responsible for creating the desired fracture length and is followed by several stages of proppant-laden fluid, which actually carry the proppant into the fracture. The closure stress of the formation causes the fracture to close; the proppants are injected to prevent this from happening. After these proppants get embedded into the fracture, a clean

fracturing fluid flushes the wellbore, commonly known as the third stage. Once the displacement of all three stages has been finished, the pumps are shut down and production is initiated. Figure 2.6 shows a typical hydraulic fracturing treatment plot.

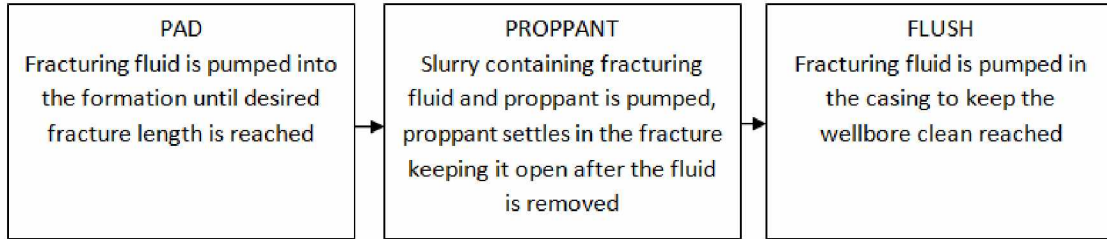


Figure 2.5 A typical hydraulic fracturing job (Beard, 2011).

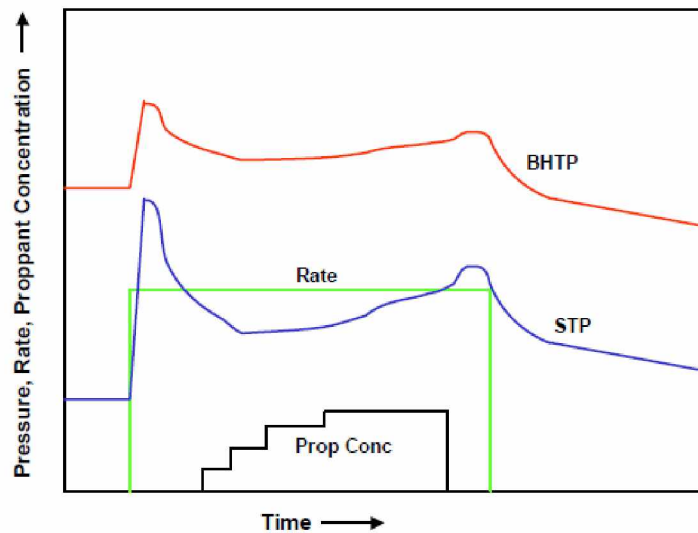


Figure 2.6 Hydraulic fracturing treatment plot (BJ Services Manual).

Hydraulic fracturing removes the skin effect of a wellbore, creating a high conductivity path that covers a long distance and extends from the wellbore to the hydrocarbon reservoir (Bukola and Aguilera, 2014). Figure 2.7 shows a non-fractured reservoir and a fractured reservoir. The upper schematic presents a wellbore with radial flow into the well, whereas the lower schematic presents a hydraulically fractured reservoir, which allows linear fluid flow in the fracture and then into the wellbore, thus contacting a larger area of the reservoir. To gain production at economic rates from reservoirs with nanodarcy permeability, it becomes necessary to integrate conventional hydraulic fracturing with horizontal drilling. Using the multi-stage fracture system, a horizontal well is placed along the target shale and fractured at regular intervals in order to attain maximum Stimulated Reservoir Volume (SRV), as shown in Figure 2.8.

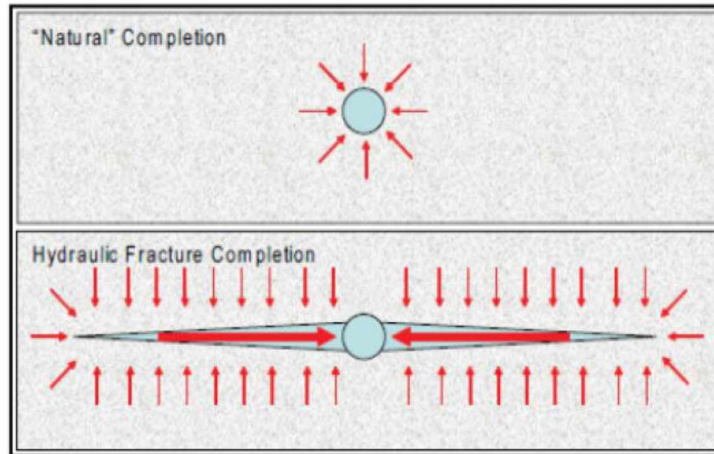


Figure 2.7 Natural completion vs. hydraulic fracture completion (Bukola and Aguilera, 2014).

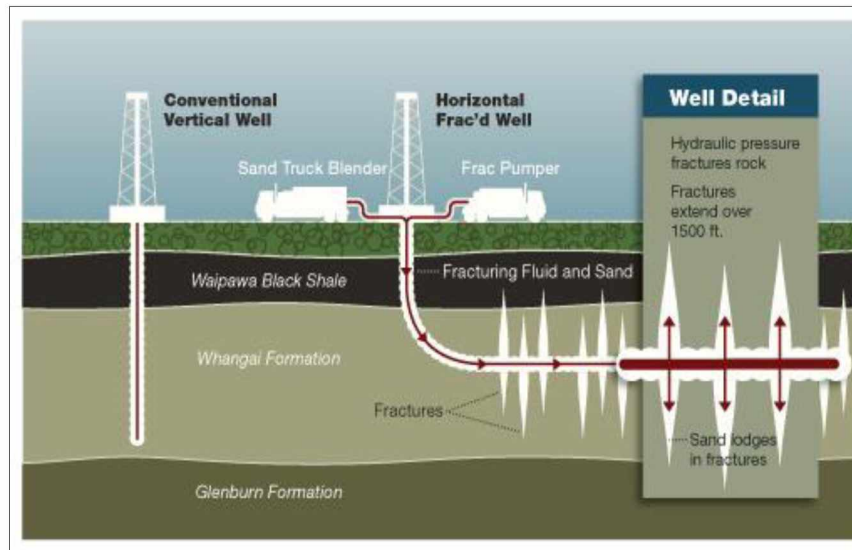


Figure 2.8 Horizontal well with multi-stage fracture technology (<http://www.tagoil.com/technology.asp#>).

Multi-stage hydraulic fracturing is carried out by isolating and fracturing the deepest segment of the horizontal wellbore, after which the depth before the deepest segment is treated. This process continues upwards until the last segment (shallowest depth) is treated (Bukola and Aguilera, 2014). Longer laterals and more stimulation stages are used to increase fracture network size and stimulated reservoir volume (Mayerhofer et al. 2008). The higher the SRV, the greater the permeability enhancement; according to Fisher and others (2004), production is directly related to the reservoir volume stimulated during fracture treatments. Thus selecting an optimum multi-stage hydraulic fracturing design can be crucial for development of any shale reservoir.

2.3 Hydraulic Fracturing Theory

This section briefly summarizes the important mechanical concepts related to hydraulic fracturing followed by engineering models for the propagation of hydraulic fractures. Fluid leak-off in fractures is also discussed, along with special considerations in designing a hydraulic fracture treatment in shale reservoirs. Classic fracturing models for rock have more or less adapted from fracture mechanics theories for metals. Most of the pioneering work for fracturing model development happened between 1950 and 1980.

Fracturing models typically combine three basic components: i) a fluid flow model; ii) a rock deformation model; and iii) a fracture propagation criterion. The fluid flow model describes pressure losses, pressure distribution along the fracture, and leak-off into the surrounding rock matrix. The rock deformation model captures the fractured surface's response to hydraulic loading. The fracture propagation criterion establishes a combination of loading and deformation conditions that result in advancement of the fracture into the intact rock volume, as shown in Figure 2.9 (Martinez, 2012).

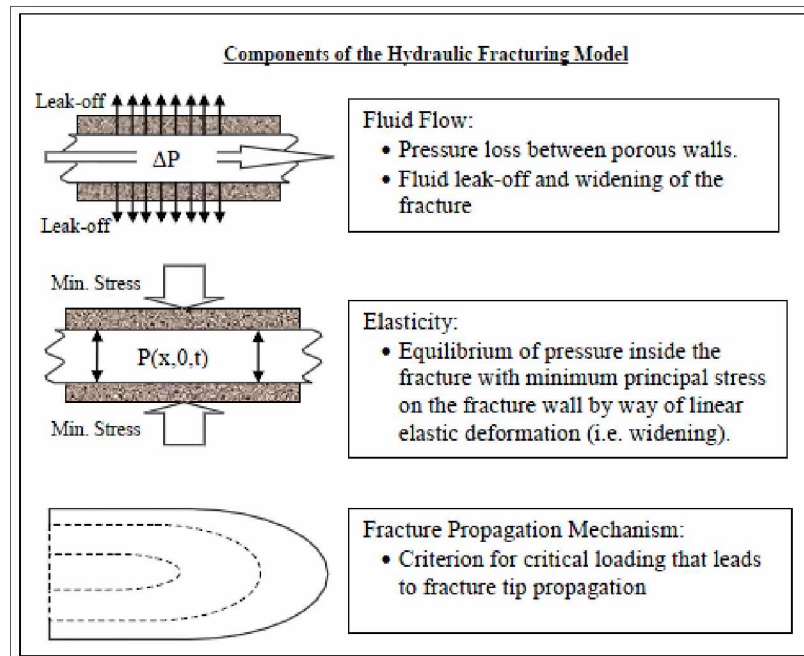


Figure 2.9 Components of hydraulic fracturing models (Martinez, 2012).

2.3.1 Multi-stage Hydraulic Fracturing

Multi-stage hydraulic fracturing refers to the process whereby multiple fractures are created along the horizontal section of the wellbore in a consecutive manner (Fig. 2.10). Multi-stage hydraulic fracturing is

carried out by isolating and fracturing the deepest segment of the horizontal wellbore, after which the depth before the deepest segment is treated; this process continues upwards until the last segment (shallowest depth) is treated (Bukola and Aguilera, 2014). This type of stimulation technique is highly efficient in shale reservoirs due to maximized reservoir contact. The subject wells of this study were completed using this type of completion technique. Completion methodology, vertical placement of horizontal wells in the formation, and the aspects of orientation and length affect the performance of a fracturing process in shales.

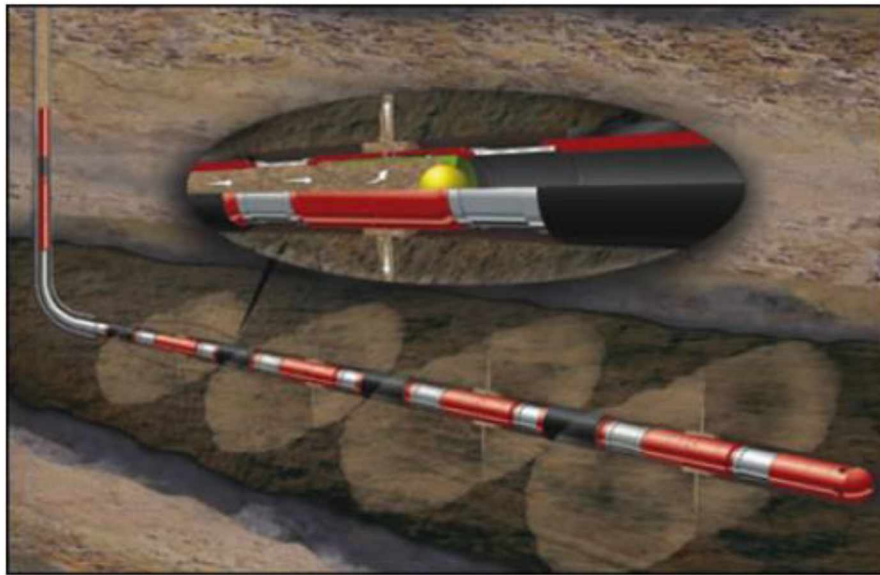


Figure 2.10 An example of multi-stage hydraulic fracturing operation: Halliburton’s Swell packer system isolating various zones of a horizontal wellbore that will be stimulated. (Bukola and Aguilera, 2014).

2.3.2 Completion Techniques

There are three types of completion techniques generally implemented in multi-stage fracturing. Plug - and-Perf uses perforations to divert the frac fluid, composite bridge plugs to isolate the fracture through the tubing, and cement to isolate the annulus of the openhole and liner string (Fig. 2.11; Kennedy et al., 2012). Ball activated systems use sleeves containing ball seats that respond to pressure and divert the frac once the sleeves are open (Fig. 2.12). Coiled Tubing-Activated systems (Fig. 2.13) use frac sleeves that are opened by means of coiled tubing; through-tubing isolation is achieved with a coiled tubing packer and annular isolation is accomplished with cement (Kennedy et al., 2012).

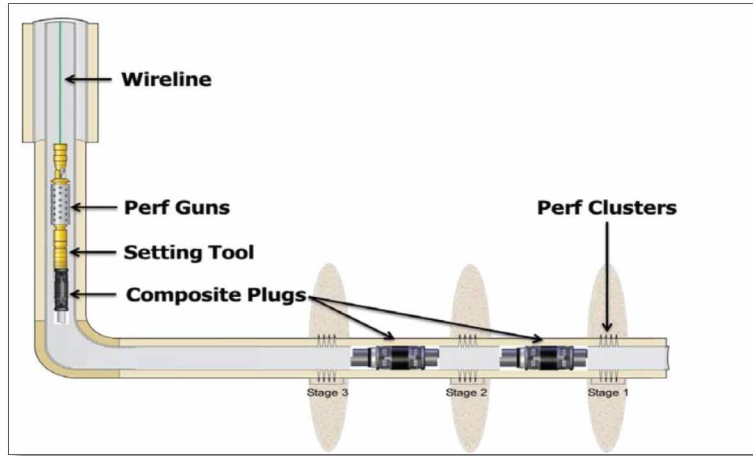


Figure 2.11 Plug-and-Perf completion system (Kennedy et al., 2012).

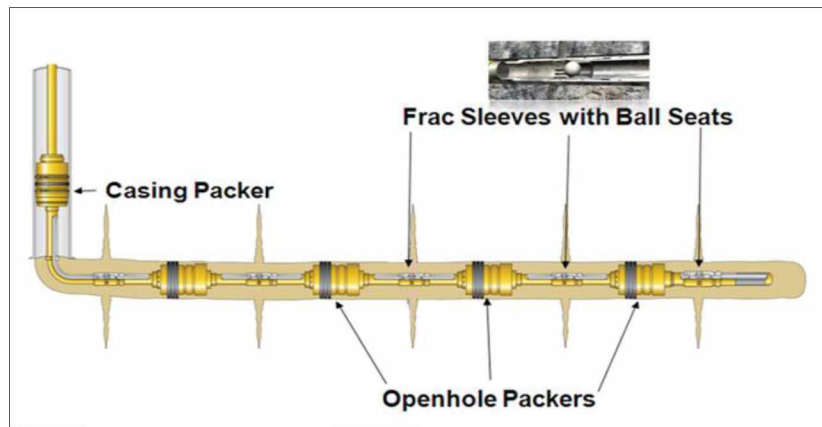


Figure 2.12 Ball activated completion system (Kennedy et al., 2012).

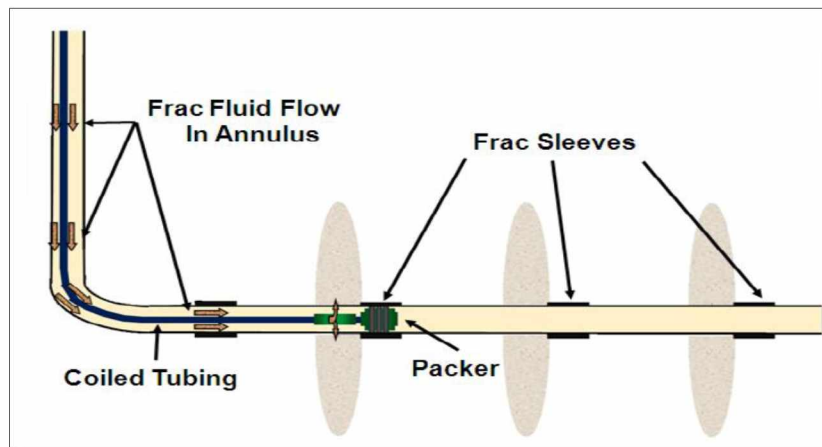


Figure 2.13 Coil Tubing - Activated completion system (Kennedy et al., 2012).

2.3.3 Fracturing Fluid Selection

Fracturing fluids play a vital role in achieving stimulation goals. These fluids initiate and help to propagate the fracture while transporting the proppant into it. Four main types of fracturing fluids were developed to meet different reservoir conditions like permeability, porosity, pressure, and temperature. The majority of hydraulic fracturing treatments use water-based fluids, oil-based fluids, foams, and emulsions. Successful stimulation is achieved when certain physical and chemical properties of fracturing fluid exist (Gidley et al., 1989):

- i) Should be compatible with the formation material and fluid.
- ii) Should be capable of suspending proppants and transporting them deep into the fracture.
- iii) Should be capable, through its inherent viscosity, to develop the necessary fracture width to accept proppant or to allow deep acid penetrations.
- iv) Should be an efficient fluid (i.e. have low fluid loss).
- v) Should be easy to remove from the formation and low friction pressure.
- vi) Should have low friction pressure and retain its viscosity throughout the treatment.
- vii) Should be cost-effective.

Stimulation operations in shale reservoirs usually require massive volumes of fracturing fluid. Water-based fracturing fluids are more widely used than oil-based mud and have various advantages. Water-based fluids are economical, incombustible, easily viscosified and controlled, usually readily available in comparison with oil-based fracture fluids, and yield increased hydrostatic head. Various additives like polymers and cross-linkers are used to improve the proppant carrying capacity of these fluids.

2.3.4 Proppant Selection and Availability

Fracturing fluid helps to propagate the fracture, but the proppant particles keep the fracture open when fluid pressure has declined after treatment. One of the first proppants used in the early days of hydraulic fracturing during the late 1940s was sand dredged from the Arkansas River (Gidley et al., 1989). Sand and resin-coated sand proppants are very common in today's shale reservoirs. Since the development of the Barnett Shale in 2004, worldwide proppant utilization increased almost 15-fold and continues to rise. With the development of new shale reservoirs, the demand for proppants has skyrocketed, straining proppant suppliers. Due to this insufficient quantity of quality proppants, many engineers compromise with the proppant selection, which affects both the fracture conductivity and production (Palisch et al., 2012).

2.3.5 Fracture Conductivity

The goal for hydraulic fracturing is to increase well productivity by altering the flow pattern in the formation and near the wellbore. As discussed earlier, propping agents keep the fracture walls apart so that a conductive path to the wellbore is retained after pumping has stopped and fluid pressure has dropped. The conductivity of the fracture can be represented by a dimensionless number, F_{CD} , which is the product of fracture permeability and fracture width. Fracture conductivity depends on properties like proppant size, strength, and grain shape, and needs to be high enough to accommodate hydrocarbon flow in the fractures. Reduction in fracture conductivity can be caused by damage factors including non-Darcy and multiphase flow, gel residue, reduced proppant concentration, fines migration, cyclic stress, and embedment (Palisch et al., 2012).

2.3.6 Methodology to Select Optimum Hydraulic Fracture Design.

Optimizing the design of a fracture treatment involves determining proppant and fracture fluid requirements, constructing a reservoir profile, determining fracture length as function of treatment size, estimating production as a function of fracture half-length, and measuring fluid efficiency and step-rate tests on site to verify design parameters. Figure 2.14 presents a general methodology for selecting the optimum fracture design. This process can be divided into two phases: pre-treatment prediction and post-treatment evaluation.

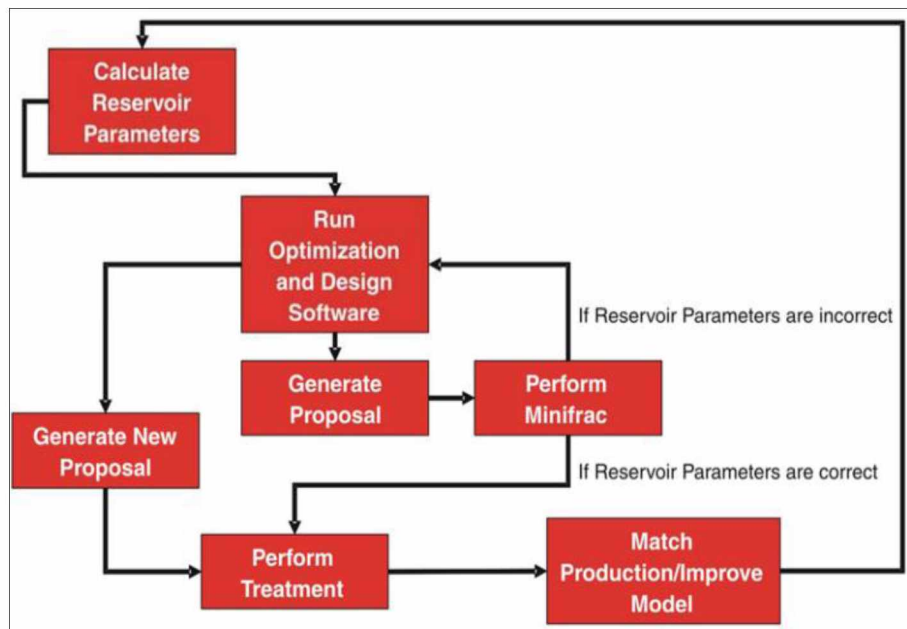


Figure 2.14 Methodology for selecting optimum fracture design (Stegent, 2004).

CHAPTER 3 Traditional vs. Modern Decline Analysis

Decline curve analysis has been used as an effective method for forecasting future production from oil and gas fields. This technique, formulated by Arps (1945) for single phase flow, is the cornerstone of production forecasting. Several different modified methods have emerged since, but Arps (1945) remains the fundamental technique to analyze production data for forecasting. The theory behind Arps Decline Curve Analysis (Arps-DCA) is to observe any decline associated with the production data and draw a curve through the data to estimate the ultimate recoverable. Arps-DCA can be termed the Traditional Analysis of forecasting, since only existing production rates and historical trends are used to predict future production rates with the implicit assumption of constant operation. Traditional Analysis is empirical in nature and it is mainly based on analogy. One advantage of traditional analysis is that it can provide production forecasts and recoverable reserves fairly rapidly. Popular techniques proposed by Arps (1945), Fetkovich and others (1987; 1996), Palacio and Blasingame (1993), Couplet and others (1994), and Agarwal and others (1999) are well documented in the literature. These techniques are designed for conventional reservoirs and primary vertical wells, and lead to two major problems when applied to tight and shale gas reservoirs (Anderson et al., 2010):

1. Pre-disposition towards boundary-dominated flow: It has been observed that linear flow is dominant in shale gas reservoirs and it takes several years for boundary-dominated flow to be observed. The traditional techniques have a tendency to under-predict the long-term performance of fractured shale gas (and tight gas) reservoirs.
2. Characterization of bulk reservoir properties: Conventional type curves assume a single fracture and associated reservoir permeability. Horizontal shale gas wells have stimulated reservoir volumes containing multiple fractures. Traditional methods do not properly capture the complexity of multi-fractured horizontal wells.

To overcome the limitations of traditional decline analysis, upgraded or modern methods have been proposed by several authors in the past 10 -12 years. These methods did exist prior to their industry-wide acceptance, but due to the lack of flowing pressure data, they were not utilized until recently. The modern methods are based on physics and are not empirical. The deliverables for modern methods are somewhat similar to those of traditional methods but more reliable, since modern methods are performance-based techniques. Using modern methods or Rate Transient Analysis (RTA), it is possible to estimate OGIP/OOIP and reserves, permeability and skin, drainage area and shape, and production optimization screening and infill potential.

The recommended approach to analyze production data from ultra-low permeability reservoirs which exhibit transient flow regimes for a long period of time is the combination of traditional and modern methods. Figure 3.1 summarizes the modern methods (RTA) as the combination of welltest analysis (pressure transient) and traditional methods (empirical). The following sections describe the different methods within RTA that were adopted to analyze the production data from the Eagle Ford's shale gas well.

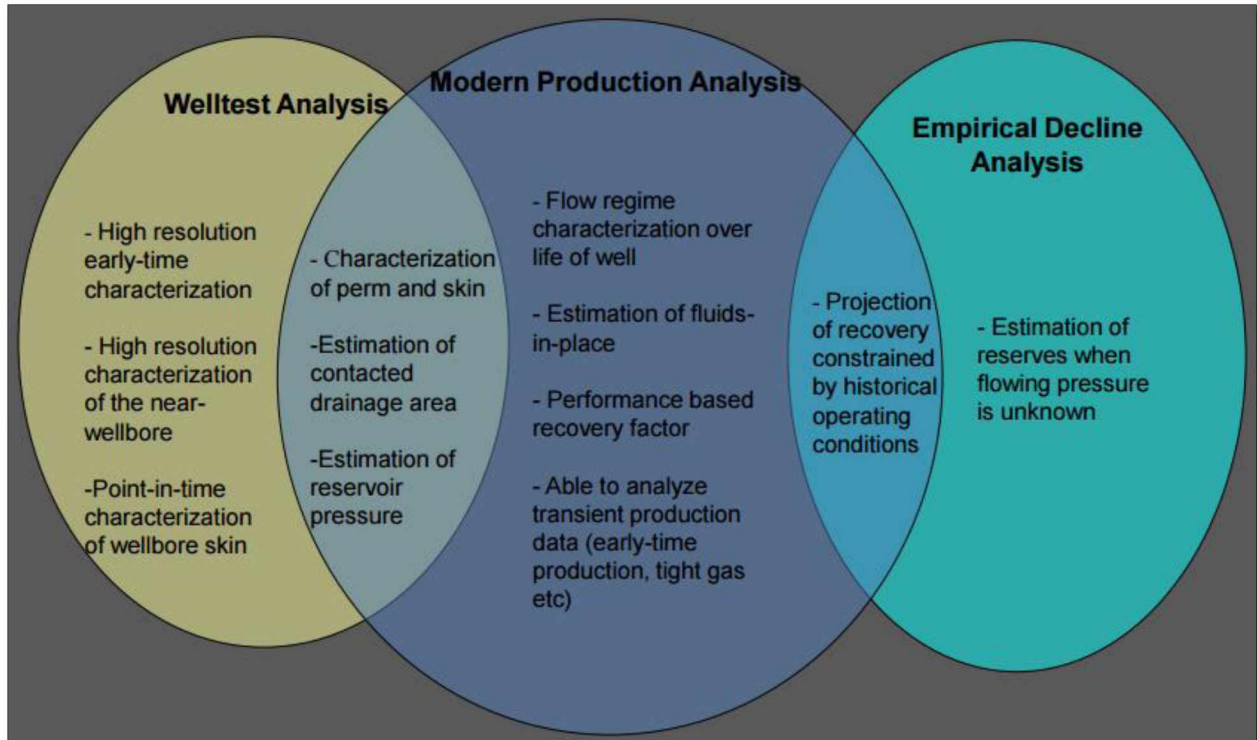


Figure 3.1 Recommended approach in terms of modern production analysis (Fekete Associates, Inc.).

3.1 Part 1 - Uncertainty in Production Data Analysis

Insight into the dynamic characteristics of a reservoir is of tremendous value to any oil and gas producing companies. Analyzing well performance data can deliver decision-making solutions regarding reserves evaluation, field development, and production optimization. Well performance analysis involves the study of the measured response of a system, the reservoir in our case, in the form of production rates and flowing pressures. Rate Transient Analysis (RTA) techniques allow the identification of a reservoir model that will appropriately describe the actual response from the system. In complex systems such as

unconventional shale plays, it is challenging to fully describe the true well-completion-reservoir system using only analytical or numerical models. This is because in wells exhibiting boundary dominated flow (BDF), RTA typically provides a reliable characterization of hydrocarbon pore volume (HCPV). However, in the presence of long-term transient flow, there is often significant uncertainty associated with those parameters, even if the quality of the history match is excellent (Anderson and Liang, 2011). In the case of unconventional reservoirs, the total HCPV is not a performance driver due to the existing low matrix permeability, hence, boundary dominated-flow cannot exist for a long period of time. In addition, the production data found in the public domain generally includes errors and discrepancies (usually due to operational inconsistencies), which makes the process of error minimization difficult and non-unique.

An integrated shale gas workflow was proposed to address the uncertainty. It involved in deriving a reasonable solution by accomplishing the minimization of an objective function that considers the difference between the simulated response and the actual response. This workflow provides a practical and efficient method for finding the best solution using an integrated method involving analytical and probabilistic approaches. The goal of this analysis is to use a systematic approach, based on RTA fundamentals and current best practices for production analysis, to obtain the best possible solution.

Mattar and Anderson (2003) presented a systematic and comprehensive approach for production data analysis, which involved using different analysis and interpretation techniques (Fig. 3.2). The workflow presented in this analysis follows the general workflow guidelines introduced by these authors. The process to conduct the analysis is straightforward and uses the steps shown in Figure 3.2. This process becomes iterative during history match of the production and pressure data using a rigorous analytical model. In addition to this general workflow, the analytical model is linked with a probabilistic approach to capture the preexisting uncertainty and verify the estimated forecasts. The probabilistic model acknowledges the existence of multiple sets of input model parameters for which a satisfactory history match is available and provides multiple realizations for both the input and output terms using simplified uncertainty modeling (Anderson and Liang, 2011).

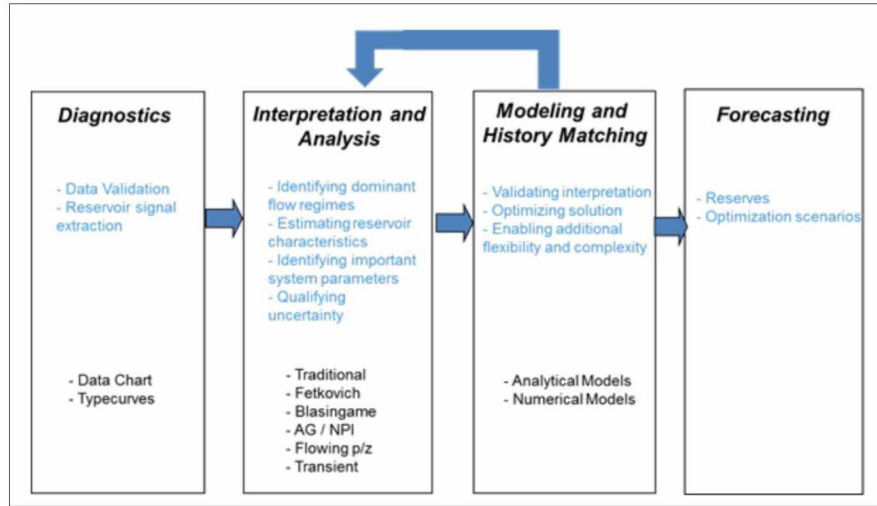


Figure 3.2 Rate Transient Analysis workflow presented by Mattar and Anderson (2003).

3.2 Pre-analysis Diagnostics

Inconsistencies in data can lead an analyst to interpret the wrong information. Most of the time inconsistencies in data become evident after the analysis has been completed. To prevent misleading answers resulting from analyzing poor quality data, a series of diagnostic plots (independent of any interpretations) are generated that will help analyze poor quality data. The production data was diagnosed in four different manners:

1. Production data outlier removal

The first step in production data diagnostics is the removal of outliers due to noise within the data. These outliers can cause incorrect interpretation if not removed along with extraneous noise in data mass. One indication of outliers was a unit slope on the type curves, which may be easily misdiagnosed as reservoir depletion, leading to misidentification of original-gas-in-place or boundary-dominated flow in the production data. Before analyzing any wells outliers were identified and removed from the analysis.

2. Liquid loading in the wellbore

It is necessary to investigate if there is any issue with liquid loading up the well, or if there is any unstable flow in the well. If liquid loading exists, and the bottomhole flowing pressure is being calculated from wellhead measurements, it is very easy to get the wrong answer, because multiphase flow calculations do not account for “stagnant” liquid columns in the wellbore. The

software calculates the bottomhole sandface pressures using the “quiet side” (i.e., the well is flowing through tubing and the pressure source is the annulus), which yields good results down to end-of-tubing. However, from the EOT to the MPP, there is often a “stagnant” liquid column, which is usually not taken into account. If the bottomhole pressure is being calculated from wellhead measurements, and the “flowing side” is being used, multiphase flow calculations must be used, and their accuracy (unless calibrated to similar flowing conditions) leaves much to be desired.

3. Single phase flow in the reservoir: check for $CGR > 100$ (bbl/scf)

Analytical models used in the rate transient analysis of production data assume single phase flow in the reservoir, which is not true for reservoirs with liquid dropout or water production. A plot of water-gas ratio versus time is used in this step. If the water-gas ratio is high, the assumption of single-phase flow in the reservoir may not be acceptable. A threshold value for water-gas ratio is defined as $CGR < 100$ (bbl / MMscf), and the portion of the data with water-gas ratio higher than the threshold value cannot be used for analysis using type curves and analytical models.

4. Consistency (correlation) between rate and pressure

After removing the outliers and the data that indicate liquid loading and productivity issues in the wellbore and/or multiphase flow inside the reservoir, it is necessary to look for consistency between pressure and rate data. If the rate and pressure data are inconsistent with each other, they should be identified and should not be used to interpret reservoir effects (permeability, skin, or gas-in-place).

3.3 Flow Regimes

The flow regime observed in tight gas or shale wells is most often linear, which may last several years and could be the dominant flow regime observed in analysis. Linear flow can be observed on square root time plots of normalized pressure with a unit slope line. This line should pass through the origin and any deviation from it will suggest the end of linear flow. For all the wells in this analysis, the square root time plot showed a negative intercept, which can lead to different interpretations. The presence of such behavior illustrated the need to consider the different flow regimes that might be at play aside from the regular ones. Ozkan and others (2009) proposed a tri-linear model that helps to broaden the scope of

possibilities. This model considers six different flow regimes over the life of the well. The flow regimes are summarized as follows (Ozkan et. al & IHS – Fekete Inc., 2007):

1. Early Fracture Linear Flow – This flow regime is the transient flow within the fractures, prior to any matrix contribution. It exhibits a $\frac{1}{2}$ slope on both the normalized rate and derivative response. This flow regime is usually very short-lived (minutes to hours) due to the low storativity and high conductivity of the fracture network. As such, it is not usually considered for practical production analysis.
2. Bi-linear Flow – This flow regime occurs after the matrix begins to contribute, but before the fracture system has reached boundary dominated flow. It exhibits a $\frac{1}{4}$ slope on both the normalized rate and derivative response. Similar to Early Linear Flow, this flow regime is temporary and unlikely to be important in daily production data analysis. In many cases, it will be masked by multiphase flow dynamics during flowback of the completion fluids, which was observed in the production data analysis. In cases where fracture conductivity is particularly high, a bi-linear flow regime may not exist at all. In these cases, fracture depletion (unit slope) will follow the early linear flow.
3. Matrix to Fracture Linear Flow – This flow regime is the transient flow from the matrix rock into the primary hydraulic fractures. It exhibits a $\frac{1}{2}$ slope. This flow regime is often dominant in fractured shale gas reservoirs and may last anywhere from days to years, depending on how closely the fractures are spaced and how permeable the reservoir rock is. If a system of secondary fractures (natural fractures activated during the completion) are connected to the primary fractures, then this flow regime will represent the flow from the secondary fractures to the primary fractures (rather than matrix to the primary fractures).
4. Transition Flow Due to Fracture Interference – This flow regime occurs after adjacent fractures begin to interfere and exhibits a slope that varies depending on the well and fracture geometry as well as the operating conditions. The range for normalized rate and derivative slope is typically between $\frac{3}{4}$ and 1 (unit slope), although it is possible for the slope to be steeper than 1. The duration of this flow regime is variable, but is related to fracture geometry and matrix permeability. In very tight reservoirs (shales) with massive fracture networks, this may be the final observable flow regime within a practical production timeframe. In more permeable tight sands with lesser fracture networks, this flow regime is much more likely to be temporary.

5. Compound Linear Flow – This flow regime is observed only after significant pressure depletion occurs within the stimulated reservoir volume and is the result of the transient linear flow from the matrix to the nominal area defining the perimeter of the stimulated reservoir volume. In the case of the tri-linear flow model, it is linear flow parallel to the fractures and into the fracture tips. As is the case with all other linear flows, it exhibits a $\frac{1}{2}$ slope. The duration of compound linear flow depends primarily on the size of the SRV in relation to the well spacing (type-curves).

6. Boundary Dominated Flow – This flow regime occurs once well interference is achieved. It exhibits a slope of 1 under constant rate, or if material balance time is used. It is exponential if constant pressure is present. This flow regime may not occur for many years and is likely not a practical consideration for shale gas reservoirs.

The Enhanced Fracture Region (EFR) Model adopted for this analysis is an effective tool for capturing shale well performance even if it does not consider the outer zone featured in Ozkan and others' Tri-Linear Flow solution. The EFR model consists of two permeability regions and can therefore still handle a change in slope, which was observed in the field data. The EFR model developed by Stalgorova and Mattar (2012) is illustrated in Figure 3.3.

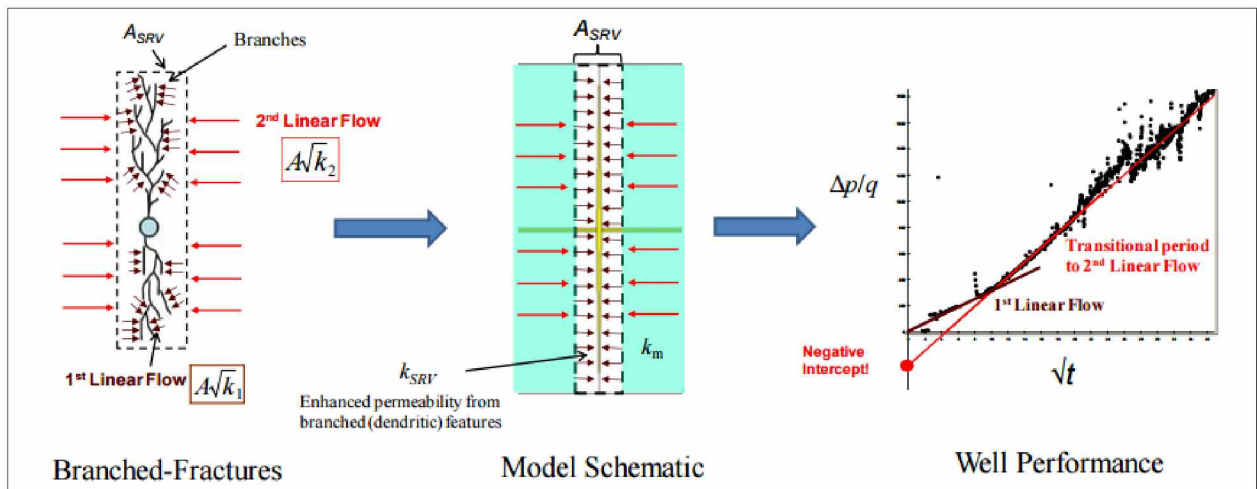


Figure 3.3 Enhanced Fracture Region Model with associated well performance profile (Thompson et al. 2012).

For early changes in slope, the EFR model is capable of different interpretations, usually a larger fracture half-length and a smaller permeability. The use of the EFR model in place of the Tri-Linear flow model is illustrated in Figure 3.4.

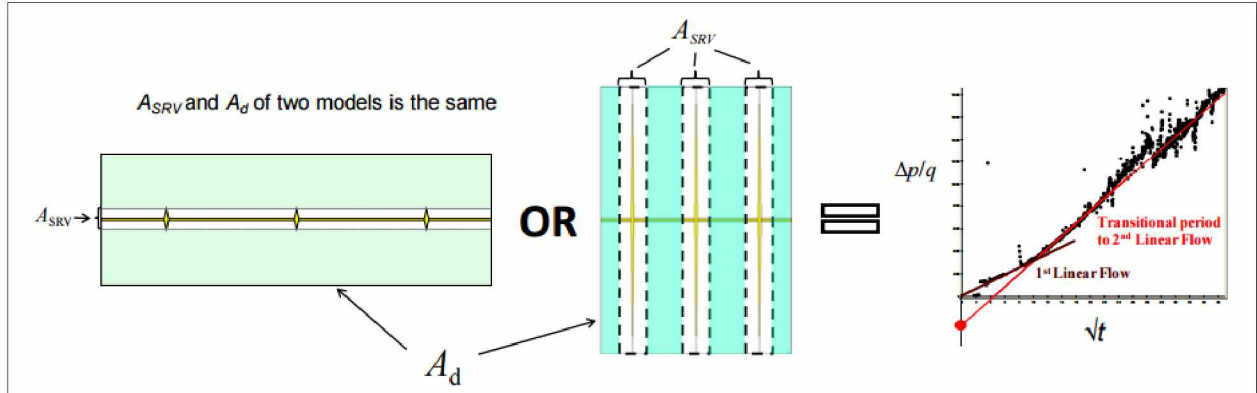


Figure 3.4 Tri-Linear Flow Model (left) vs. Enhanced Fracture Region Model (right) (Thompson et al. 2012).

For the data analysis in this work, almost all wells exhibited negative intercepts on the square root time plot. To identify if a straight line passed through the origin or had a negative intercept, a small square root time plot analysis was conducted. From this analysis it was observed that if the straight line passed through the origin it usually overestimated the A_{SRV} (80 acres), whereas a negative intercept gave reasonable values for A_{SRV} (36 acres), as illustrated in Figure 3.5.

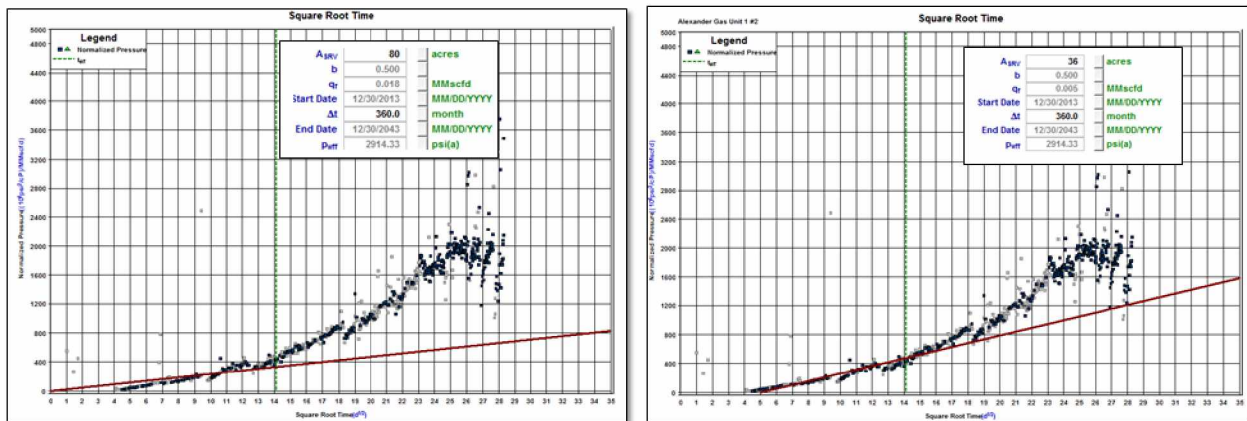


Figure 3.5 Square Root Time plot analysis passing through origin and negative intercept (Fekete Associates Inc.).

The reason for overestimation in the stimulated area volume was due to the calculated fracture half-length. The less steep slope of the straight line passing through the origin estimated a higher fracture half-length, which gave a higher stimulated area. In order to correct for this overestimation, the straight line

was allowed to pass through the negative intercept. To be consistent throughout the analysis, the straight line was allowed to have a negative intercept. Anderson and others (2012) summarized several possible causes for negative intercepts. The ones that applied to this analysis based on observation and data quality are as follows:

- Failing to calculate the correct bottomhole flowing pressure (liquid loading)
- Linear flow with pressure dependent effective permeability (Thompson et al.,2010)
- Increasing skin damage over time (e.g. phase trapping, salt precipitation, wax deposition, etc.)
- Offset well completions (well interference effects)
- Plotting early shut-in data (days with-no production), transposes the linear flow straight line to the right
- Second linear flow period caused by complex branched or dendrite fractures, as shown in Figure 3.3.

The bulk of production data for most wells was represented by a transitional period following early linear flow. Allowing the straight line to pass through the negative intercept made it visually consistent in determining the end of linear flow.

3.4 Flowing Material Balance Analysis Theory

The flowing material balance is one of the newly adopted methods in RTA. It uses actual reservoir performance data and can be considered an accurate procedure for estimating Original Hydrocarbon in Place (OHIP). The traditional material balance plot requires the well to be shut-in at several producing times to obtain an average reservoir pressure. This requirement is considered impractical from an economic standpoint and the duration of the shut-ins is often not long enough to obtain accurate measurements. The flowing material balance theory uses the flowing pressures and rates to calculate OHIP under the concept of boundary-dominated or pseudo-steady state flow.

3.4.1 Pseudo-Steady State

A well reaches boundary-dominated flow after it has “felt” all the boundaries. Behavior of such wells is governed by pseudo-steady state equations. Under the assumption that the flow rate of the well is constant, the pressure at all locations in the reservoir will decline at the same rate. Once pseudo-steady state is reached the well, the drop in average reservoir pressure would be constant at any given point between the wellbore and the reservoir boundary (Figure 3.6).

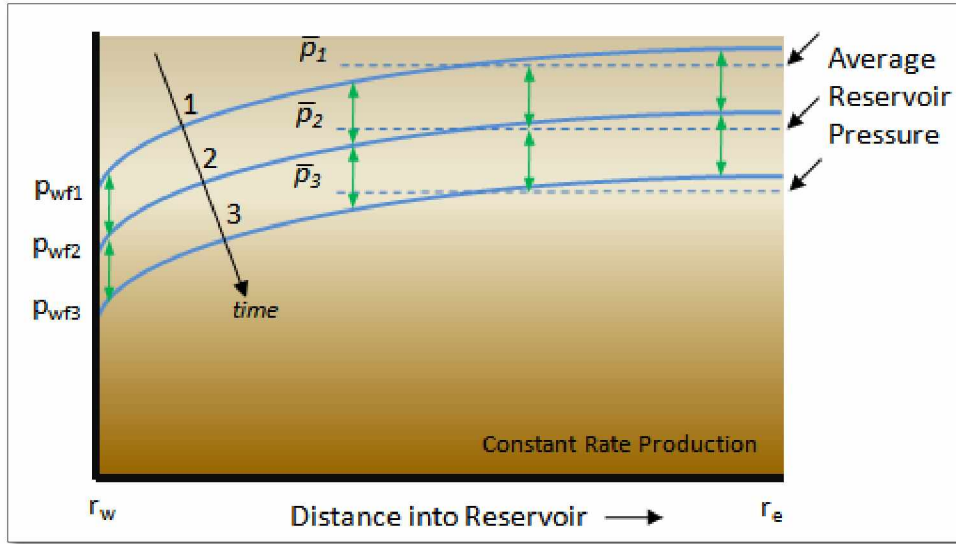


Figure 3.6 Pseudo-steady state conditions for a given well (Fekete Associates Inc.).

The P/z plot or the material balance plot was introduced for estimating original gas in-place. A conventional plot uses the extrapolated straight line of measured shut-in pressures to predict OGIP. The same methodology is applied to flowing pressure, under the assumption of constant rate boundary-dominated flow. The following equation is the pseudo-steady state equation for vertical gas wells in the center of a circular reservoir (D. Anderson & P. Liang, 2011):

$$\Delta P_p = P_{pi} - P_{wf} = \frac{2qp_i t_a}{(\mu c_t Z)_i} + \frac{1.147 \cdot 10^6 T}{kh} \left[\ln \frac{r_e}{r_{wa}} - \frac{3}{4} \right] \dots \dots \dots (\text{Eq. 1})$$

The above equation can be modified for use in horizontal wells with multiple fractures. Figure 3.7 shows a material balance plot (p/z vs. G_p), where p_{wf}/z is the flowing sandface pressure at the wellbore vs. cumulative production. The plot illustrates a straight line drawn through the flowing sandface pressure data. This line is then extrapolated from the initial reservoir pressure, which estimates the original gas in place. Making the line pass through initial p/z point does not change the slope and makes material balance analysis possible without shutting-in the well.

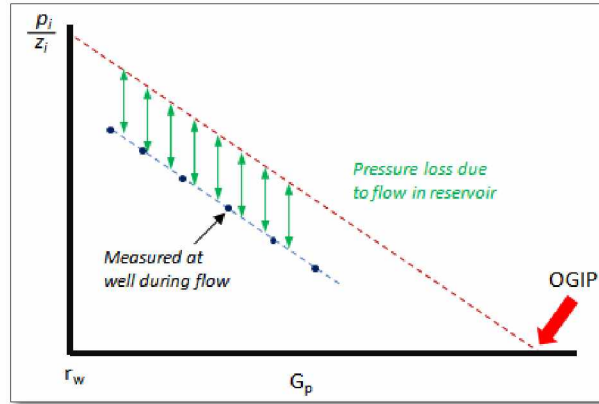


Figure 3.7 Flowing Material Balance Plot (Fekete Associates Inc.).

3.5 Analytic Model – The Enhanced Fracture Region Deterministic Model

Analytical models are used to validate interpretations and provide production forecasting. They assume single-phase flow in the reservoir. Modeling is the process of history matching pressure and rate transient data based on a mathematical model. Each situation presents a unique solution to which there are many different models available to match the data. Analytical models are not unique, i.e., different model types can match the same set of data, and as a result, it is recommended that the choice of model type occur after the analysis step. In analytical modeling, parameter values obtained during the analysis step provide a good starting point for an appropriately chosen model type. Automatic parameter estimation was used to optimize generated parameters in the Unconventional Reservoir model analysis. The pre-analysis diagnostics discuss more about corrupted data, outliers, and noise in the data.

The analytical model adopted for this analysis was developed by Stalgorova and Mattar (2012). It is an extension of the tri-linear flow solution, subdividing the reservoir into five regions. The model simulates a fracture that is surrounded by a stimulated region of limited extent (bench-fracturing) with the remaining reservoir being un-simulated. The model is also capable of considering the flow from the surrounding un-stimulated region, both parallel and perpendicular to the fracture. This is in addition to modeling flow within the fracture and flow within the stimulated region.

In tight reservoirs with multi-frac horizontal wells, fractures do not have a simple bi-wing shape but are branched as shown in Figure 3.8. Daneshy (2003) proposed that in many cases propagation of a fracture creates a branch pattern. This branching introduces a region of high permeability around the fractured region. This model considers five regions of linear flow and encompasses both the tri-linear solution suggested by Brown and others (2009) and the Enhanced Fracture Region Model presented by Stalgorova

and Mattar (2012). The authors derived a solution for the schematic, shown in Figure 3.8, and called it the Five Region Model, also referred to as the Enhanced Fracture Region Model.

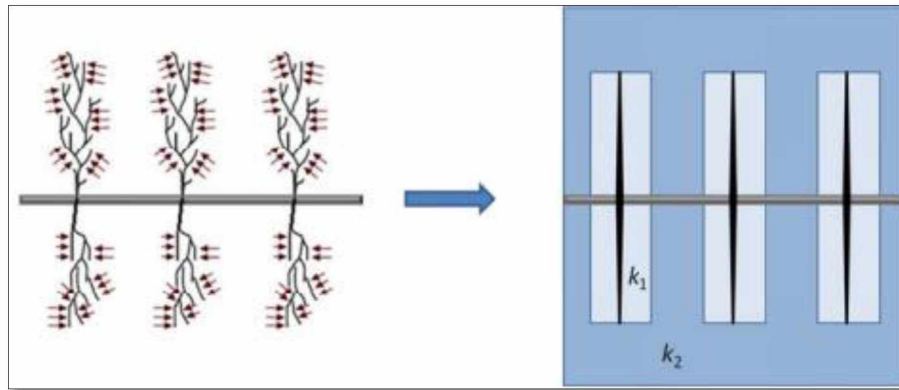


Figure 3.8 Horizontal well with multiple branch fractures (left) and its representative model (right), $k_1 > k_2$ (Stalgorova and Mattar, 2012).

It was assumed that all fractures have the same length and conductivity with uniform spacing along the horizontal well. The portion of the reservoir around the fracture is defined as the enhanced permeability region and its distance from the center of the fracture is given by X_{1i} , as illustrated in Figure 3.9. Stalgorova and Mattar (2012) assume symmetry of the system and perform calculations on one quarter of the space between the fractures. Figure 3.10 illustrates the flow in the model, which is treated as the combination of five linear flows within contiguous regions. Each region is formulated with 1-D flow solutions and then coupled by imposing flux and pressure continuity across the boundary between regions. The model consists of regions 1 to 4 and the fracture region, as shown in Figure 3.9. Petrophysical properties like porosity, permeability, and compressibility are assumed constant for regions 2, 3, and 4, as those regions represent the matrix. These properties are varied for region 1, as it represents the enhanced permeability region near the fracture. Derivation for this model is presented in the Appendix.

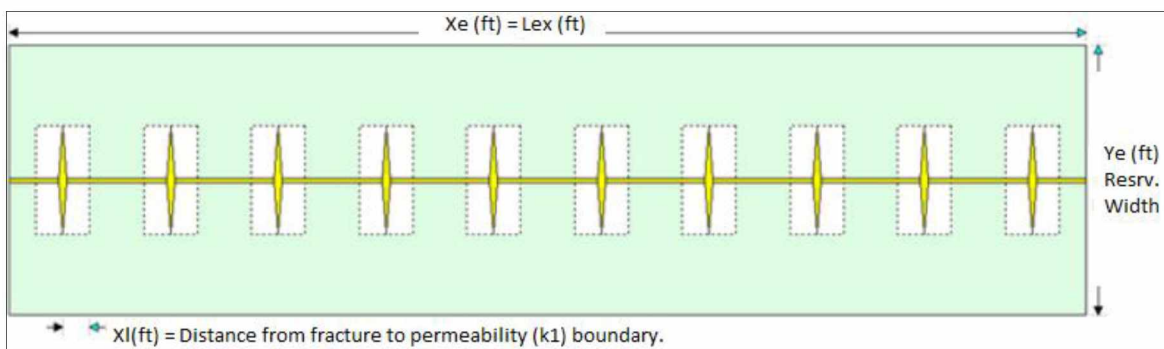


Figure 3.9 Enhanced Fracture Region Model Schematic (Fekete Associates Inc.).

This model takes the following linear flow regimes into account:

- Linear flow within the fracture (at very early time of production)
- Linear flow within stimulated region towards the fractures
- Linear flow within the non-stimulated regions towards the stimulated region
- Linear flow within the non-stimulated region towards the wellbore

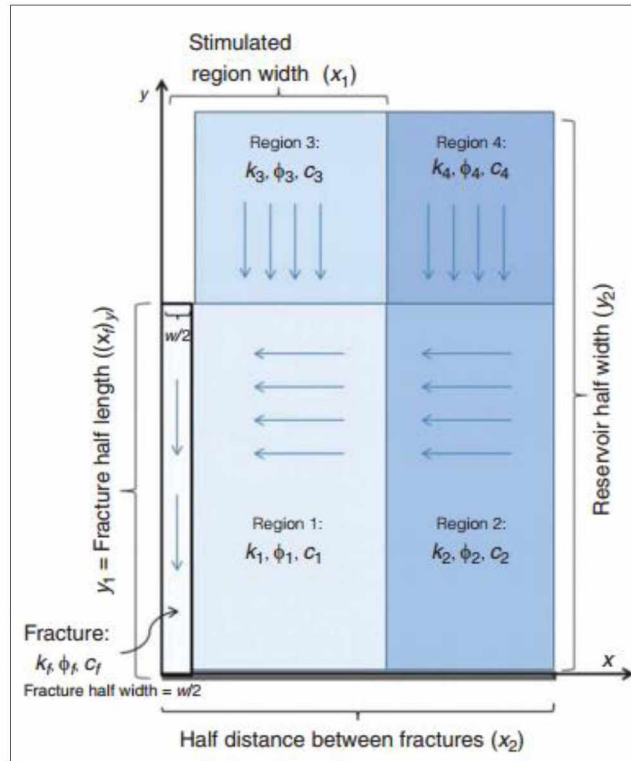


Figure 3.10 Schematics and dimensions for the five-region model (Stalgorova and Mattar, 2013).

This model was derived initially for a liquid system, but Stalgorova and Mattar (2012) proposed that real-gas pseudopressure should be used for dimensionless pressure. The commercial software used for this analysis adopts this model and makes the required corrections for the appropriate fluid type and reservoir.

3.6 Uncertainty Modeling & Modified Workflow

The aforementioned analysis type and model serve the purpose of forecasting production and determining expected recovery. The resolution of a reservoir's bulk to explicit physical characteristics is challenging, since it involves the solution of an inverse problem. Since most of the interpretation is conducted based

on the bulk production data, which is dominated by transient flow, especially in the case of shale gas wells, a significant degree of uncertainty is introduced, making the approach not deterministic. The models require an application of inverse solution by history matching, which even when achieved will yield a non-unique solution. This is because of the complexity of the reservoir and due to the number of existing unknown parameters. To address this uncertainty, a probabilistic approach has been adopted.

A probability analysis using Fekete's RiskTM analysis model was conducted on the results achieved using the Analytical Enhanced Fracture Region model. The first step in conducting the RiskTM simulation was to define probability distribution for a set of unknown modeling parameters. For this analysis 100 simulation runs were performed, where each run randomly sampled values for the modeling parameters and calculated discrete forecast and reserve estimates. This helps to address the uncertainty in multiple input parameters, whereas the deterministic model requires single inputs. Three options were considered to assign uncertainty to parameters: assign a distribution (uniform or triangular), hold the parameter constant, or allow the parameter to be calculated based on other input.

Parameters that did not represent any uncertainty, mostly petrophysical and reservoir parameters, were held constant. Uniform distribution allowed the random sampling of parameters with lower and upper limits. The assumption behind these limits is discussed in later sections. A triangular distribution was only assigned to the 'number of fractures' (n_f) parameter. Due to the lack of microseismic data, it is impossible to know how many fractures are operational at any given time in the well's life. The best approach to this issue was assigning a triangular distribution, which also has lower and upper limits, with the sampling weighted towards a best estimate that lies in between (i.e., mode). The rest of the parameters which held the majority of the uncertainty, mainly x_f (ft) and k_{sv} (nD), were assigned Automatic Parameter Estimation (APE). The APE option attempts to minimize the difference between the synthetic curve and the historical data by modifying the selected parameter. This option allowed honoring the history match but reduced the randomness of the process.

Upon completion of the runs, the results were aggregated and the data was analyzed statistically. The stochastic results include a set of P10, P50, and P90 forecasts, along with distribution plots for in-place volumes and reserves. The forecast results were then compared with the analytical model result. If the values fell within a 10% range of each other, the solution was considered reasonable, otherwise an iterative process was followed until the acceptable range was achieved. Adopting the probabilistic analysis in addition to Mattar and Anderson's (2003) RTA workflow introduces a modified process for analyzing well performance data and generating forecasts.

3.7 Procedure

IHS-Fekete’s Harmony software was used to conduct a Rate Transient Analysis on the Eagle Ford shale gas wells. Within the software, the IHS-RTA™ suite was implemented to conduct most of the analysis on the wells. Figure 3.11 shows an illustration of the initialization data that is put in the software, allowing the user to begin RTA.

The operator company provided the following data for all the wells:

- Reservoir and PVT data
- Petrophysical data
- Production data with flowing pressures
- Wellbore schematic with deviation survey
- Wellhead pressures converted to sandface pressures using the software’s default Gray’s pressure-loss correlation.

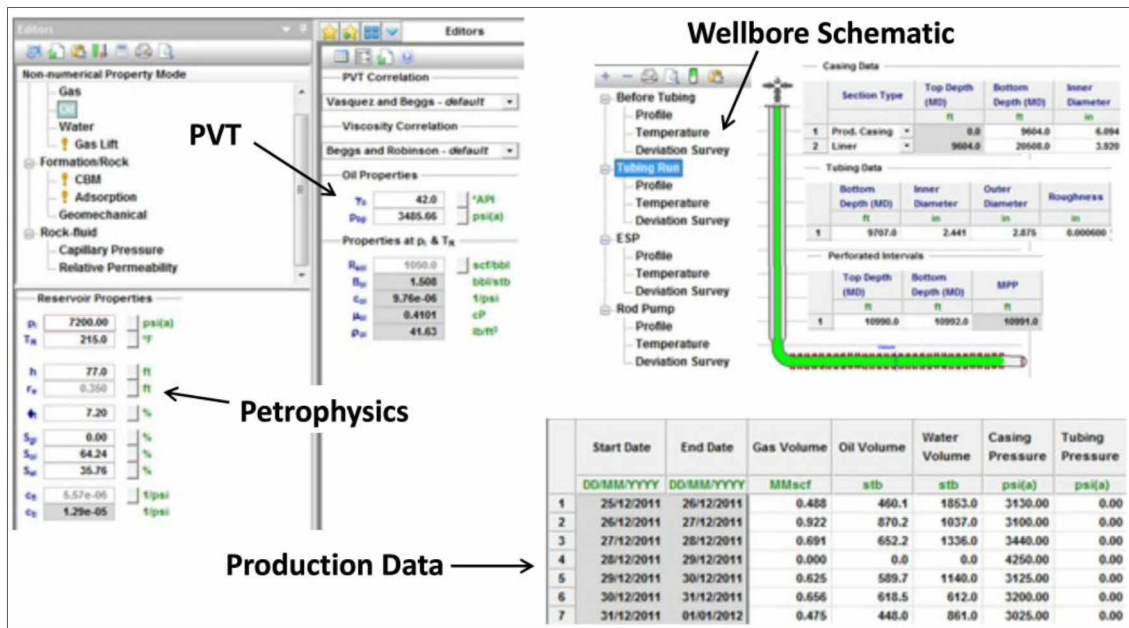


Figure 3.11 IHS-RTA software schematic for initialization data.

3.8 Base Case: Reservoir Width = 1500 ft.

A base case was considered for this analysis, with an assumed reservoir width of 1500 ft . This is based on the assumption that the well spacing and the reservoir boundary for each well are unknown. A typical single well without any nearby lateral will have about 1500 ft of reservoir boundary in the Eagle Ford shale reservoir (Portis et al., 2013). This assumption also allows the well to behave as if it had an infinite

boundary. This is due to the effect of ultra-low matrix permeability. This assumption was applied to all the wells and the integrated process is as follows:

1. At the first stage of the analysis, the Variable Pressure Plot is used to estimate the Stimulated Reservoir Volume and fracture half-length by identifying the deviation from a straight line. This is the minimum stimulated reservoir volume area seen by the well and the corresponding fracture half-length, as shown in Figure 3.12.
2. This minimum A_{srV} is reflected in the Superposition Time Plot along with the other reservoir parameters. The Superposition Time plot is utilized to replace the Variable pressure plot since it helps to filter noise from the data by linearising the variable rates.
3. The number of fractures was estimated based on a most-likely approach proposed by Anderson and Liang (2011). The idea behind this methodology is to identify a specific parameter space for a certain stimulated reservoir volume configuration based upon the known minimum and maximum input parameters (Figure 3.13). In this case, minimum and maximum values for number of fractures and matrix permeability were used as inputs. The minimum number of fractures was assumed to be one operational fracture per stage, whereas the maximum number of fractures was assumed to be working at 90% efficiency times the number of clusters per stage. The matrix permeability constraint was set between 10 nD and 100 nD. This range was adopted based on operator suggestions and those described by Mullen (2010) in his work.
4. The EFR analytical model is seeded with petrophysical properties along with physical reservoir parameters such fracture half-length (x_f), number of fractures (n_f), and a reservoir width (Y_e) of 1500 ft. The model is run to conduct a pressure history match by iterating on stimulated reservoir permeability (k_{srV}), reservoir matrix permeability (k_m), dimensionless fracture conductivity (F_{cd}), and X_L (ft). The constraints for the above parameters are shown in Table 3.1. The reservoir matrix permeability is constrained between 10 – 100 nanoDarcy (nD), as described by Mullen (2010). Anderson and Thompson (2014) suggested that dimensionless fracture conductivity can be evaluated as infinite due to the effect of ultra low matrix permeability. It was constrained to be less than 2000 based on the suggestions made by the operator. The analytical model-introduced parameter X_1 was constrained between 5 ft and half of the cluster spacing, which was also based on suggestions made by the operator.

Table 3.1 Parameters and their respective constraints within the EFR analytical model

Parameters	Constraints
k1 (nD)	NA
k2 (nD)	$10 < k2 < 100$
Fcd	$Fcd > 2000$
Xl (ft)	$5 < Xl < (\text{Cluster Spacing} * 0.5)$
Ye (ft)	1500

5. The results obtained from the EFR analytical model were used as input in the probabilistic model. The probabilistic model utilizes Monte Carlo simulation to generate multiple model history matches and associated forecasts within a predefined parameter space provided by the analytical model. The advantage of this approach is that it addresses the uncertainty in multiple input parameters simultaneously through random sampling. While assigning uncertainty to each parameter, three options were considered: assign a distribution (uniform or triangular), hold the parameter constant, or allow the parameter to be calculated based on other input. Parameters with uniform distribution were sampled randomly between prescribed lower and upper limits. Uniform distribution was applied to k_2 (matrix permeability, nD), X_L (ft), and Y_e (ft). The number of fractures was assigned a triangular distribution to weigh the sampling towards a best estimate that lies in-between the lower and upper limit (i.e., the mode). Auto Parameter Estimation (APE) was assigned to the parameters with the most uncertainty, such as x_f , F_{cd} , and k_1 . Table 3.2 summarizes the distribution inputs for all the parameters. A total of 100 simulation runs were conducted for each well.

Table 3.2 Uncertainty distribution for each parameter within probabilistic modeling

Parameters	Distribution	Min	Mode	Max
Pi (psia)	Constant	-	-	-
xf (ft)	APE	-	-	-
Fcd	APE	-	-	-
nf	Triangular	$nf * 0.3$	$nf * 0.6$	$nf * 0.9$
Le (ft)	Constant	-	-	-
k1 (nD)	APE	-	-	-
k2 (nD)	Uniform	10	-	100
Xl (ft)	Uniform	5	-	(Clust.Spac)/2
Ye (ft)	Uniform	500	-	1500
h (ft)	Constant	-	-	-
ϕ (%)	Constant	-	-	-
Sg (%)	Constant	-	-	-
So (%)	Constant	-	-	-
Sw (%)	Constant	-	-	-
cf (1/psi)	Constant	-	-	-
CGR (bbl/Mmscf)	Constant	-	-	-

6. Results from probabilistic analysis were compared to analytical forecast results and if the percent difference within the EUR values was less than 15%, the analysis was considered valid. If the percent difference was greater than 15%, the entire analysis was re-conducted until the threshold value condition was satisfied. This process is illustrated in the modified workflow shown in Figure 3.14.

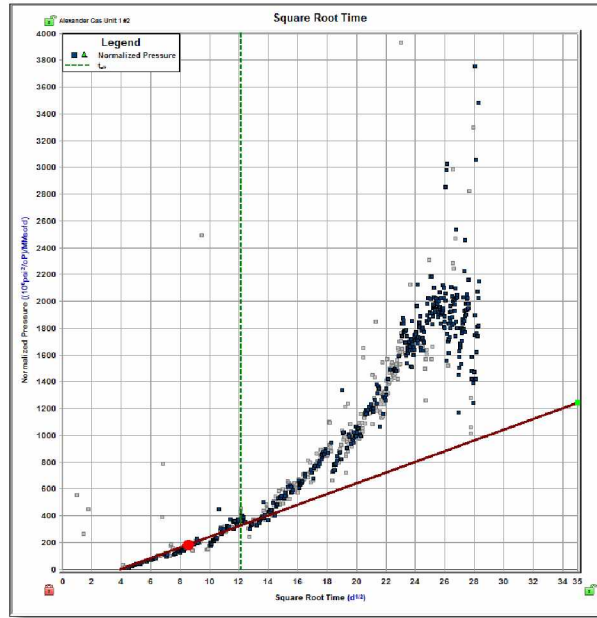


Figure 3.12 Square Root Time plot in the Unconventional Model (Fekete Associates Inc.).

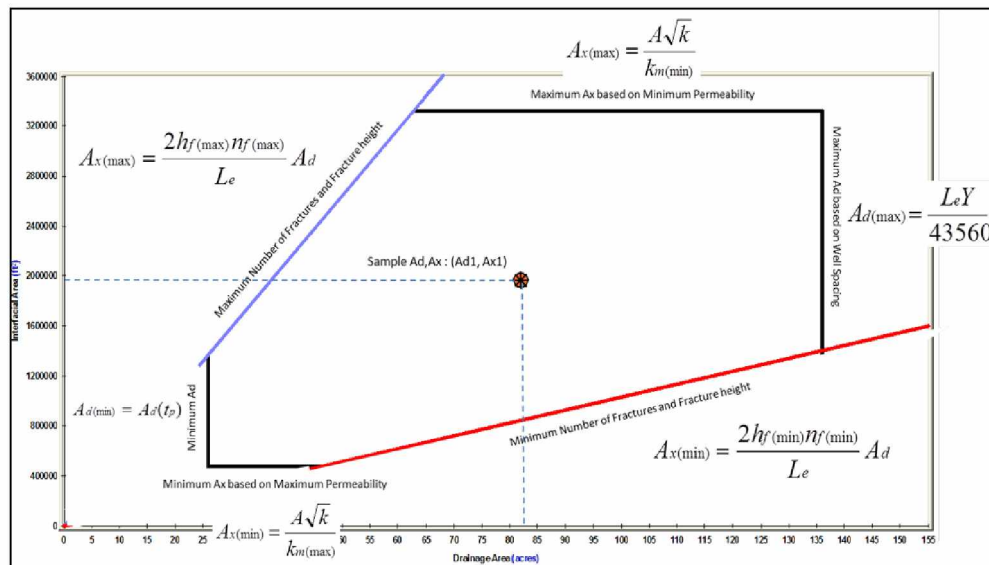


Figure 3.13 Schematic for the Most-Likely Approach (Fekete Associates Inc.).

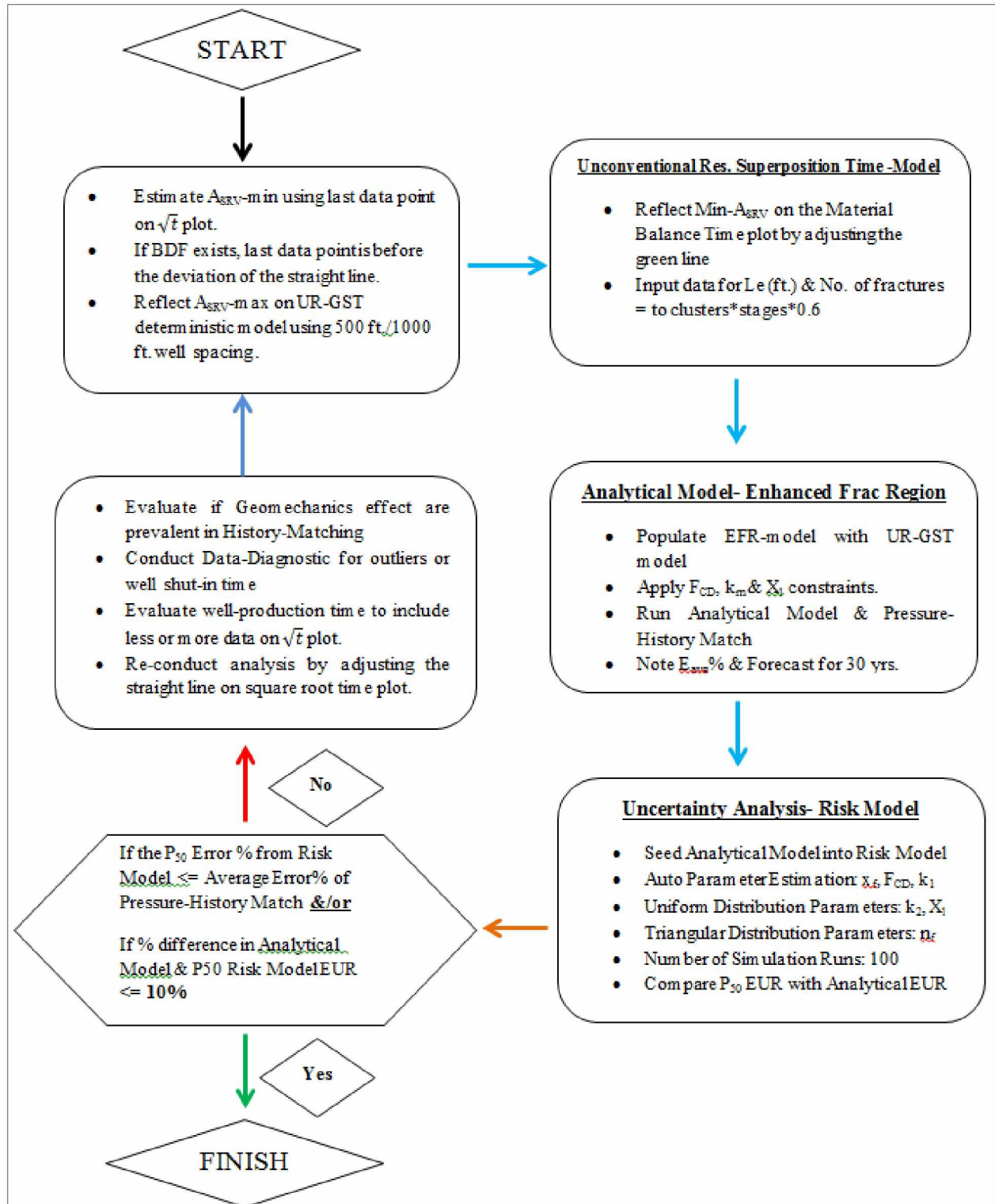


Figure 3.14 Modified workflow adopted for this analysis.

3.9 Data Analysis & Results

The operator provided total of 21 wells upon which to conduct the analysis. Out of those 21 wells, only 16 were analyzed. Table 3.3 lists well numbers and types. The breakdown for selecting wells for this analysis is as follows:

- Total Wells = 21
- Oil Wells = 2
- Suspended Gas Wells = 3
- Wells Analyzed = 16.

Table 3.3 List of provided wells for analysis. Only gas wells were analyzed (in blue).

Sr. No	Well Name	Well Type
1	A	Gas Well
2	B	Suspended Gas Well
3	C -1	Gas Well
4	C-2	Gas Well
5	D	Gas Well
6	E-1	Suspended Gas Well
7	E-2	Gas Well
8	F	Gas Well
9	G	Gas Well
10	H-1	Suspended Gas Well
11	H-2	Gas Well
12	I	Gas Well
13	J-1	Oil Well
14	J-2	Oil Well
15	K	Gas Well
16	L	Gas Well
17	M	Gas Well
18	N	Gas Well
19	O	Gas Well
20	P	Gas Well
21	Q	Gas-Well

3.10 Deterministic & Probabilistic Results

Tables 3.4 and 3.5 summarize the deterministic and probabilistic results for all the wells that were analyzed using the integrated approach. From the comparison of the results, it is clear that the deterministic approach consistently overestimates the A_{SRV} (acres). There was a reasonable agreement between the fracture half-length values for both the analyses. Figure 3.15 shows a bar chart for different fracture half-length values for each well using both approaches. It is evident from this chart that fracture half-length values are within a reasonable agreement ($100 < x_f < 200$ ft.) of each other, except for Well E-2. These results validate the consistency achieved using square root time plots to estimate fracture half-length (x_f). On average, k_1 (nD) values were always overestimated by the probabilistic analysis, as shown in Figure 3.16. Matrix permeability (k_2) values were more or less within a range since a lower and upper limit of 10 (nD) and 100 (nD) was applied based on operator feedback and literature review. The model-based parameter X_1 was also within a reasonable range for both the approaches. Since k_2 and X_1 had uniform distribution, the probabilistic analysis randomly sampled mostly P50 values or the mode of the provided range. The forecast generated by deterministic analysis matched fairly with the P50 forecast from probabilistic analysis. This is depicted in the plot of deterministic vs. probabilistic (P50) EUR forecast, where almost all the values lie on the forty-five degree line shown in Figure 3.17.

The EUR results confirm that the production analysis conducted for the Eagle Ford shale gas wells is reliable in terms of long-term forecasting. The lowest 30 year EUR forecast was around 800 (MMScf) for Well C-1, which indicates that this well was drilled in a rich-condensate zone and which is confirmed by its high condensate to gas ratio (361 bbl/scf). The highest 30 year EUR forecast was generated for Well-G and Well-I, around 3500 (MMScf). These two wells had also been producing the longest and might be getting some contribution from beyond the SRV region. There are two explanations for this hypothesis. Either the well-spacing assumed for the base case is too large and wells are closely spaced to experience boundary-effects, or the assumed matrix permeability is not representative of the formation (too small) in which these wells are drilled. Since most of the wells did not show any signs of deviation from the straight line on the square-root time plot, total drainage volume or the actual boundaries are still decades away from being observed. The biggest ambiguity lies within the absolute recovery from these wells which can be directly related to the uncertainty in volumetric and well spacing. Both the deterministic and probabilistic approaches provided accurate and consistent production forecasts and EUR. This may indicate that beyond some certain minimum value, Ultimate Recovery might have a low sensitivity to total drainage volume. If EUR forecasting is the sole goal of an analysis, the proposed integrated method is a consistent approach to conduct the analysis.

Table 3.4 Deterministic results for all wells

Deterministic											
Well Name	Asrv (acres)	Ad (acres)	xf(ft)	Fcd	nf	k1 (nD)	k2 (nD)	Xl (ft)	Ye (ft)	EUR (Mmsecf)	Pressure-History Match Avg. Error.
A	29	168	131	1907.3	33	9992.2	64.97	35	1500	2974	28.309
C -1	32	140	171	1924.8	35	702.74	62.78	25	1500	764	2.281
C-2	40	245	161	355.4	37	204.64	43.24	38	1500	1147	4.841
D	27	175	115	1990.7	26	145.87	23.27	27	1500	3204	13.224
E-2	42	165	193	1996.5	41	9999.9	99.9	32	1500	1861	2.483
F	21	128	128	1962.1	21	9999.6	48.35	33	1500	2759	26.261
G	30	201	111	2.7	40	9999.9	100	32	1500	3668	4.928
H-2	23	113	150	587.5	23	1349.8	63.97	30	1500	2261	32.533
I	17	145	107	218.4	39	339.52	22.29	30	1500	3117	30.44
K	25	190	100	121.3	34	1732.4	21.34	34	1500	3229	22.183
L	23	192	171	1978.7	40	242.58	26.67	32	1500	1966	1.405
M	24	132	132	1641.4	26	1289	49.06	29	1500	3151	11.979
N	27	147	139	24.9	29	1074.9	16.99	32	1500	1400	16.78
O	27	165	122	200.6	39	9995.4	31.51	34	1500	1506	9.911
P	29	138	157	1901.2	42	9199.9	13.81	22	1500	2543	34.3
Q	30	200	113	511.7	46	1118	99.99	28	1500	1727	3.051
Minimum	17	113	100	2.7	21	145.87	13.81	22	1500	764	1.405
Maximum	42	245	193	1996.5	46	9999.9	100	38	1500	3668	34.3
Average	27.875	165.25	137.563	1082.8	34.438	4211.6	49.2588	30.8125	1500	2329.813	15.3068125

Table 3.5 Probabilistic results for all wells

Probabilistic (P50)											
Well Name	Asrv (acres)	Ad (acres)	xf(ft)	Fcd	nf	k1 (nD)	k2 (nD)	Xl (ft)	Ye (ft)	EUR (Mmsecf)	Avg. Error.
A	11	114	176	1913.1	39	9659.2	56.8	20	1020	3034	53.574
C -1	12	94	201	1904.2	39	713.12	55.27	18	1003	790	3.023
C-2	15	164	152	959.6	51	9630	55.25	23	1002.5	1116	5.034
D	3	116	46	1255.7	42	9811.2	54.68	46	996.5	3300	64.81
E-2	21	112	302	1936.8	45	9512.6	56.08	19	1012	2009	3.018
F	6	85	117	1937.7	33	9997.6	55.18	19	1002	2582	37.721
G	14	134	159	16.2	54	1519.7	55	19	1000	3412	5.311
H-2	9	76	109	490.5	45	755.31	55.54	19	1006	2116	50.269
I	7	97	131	714.3	34	9896	55.09	18	1001	3552	102.87
K	5	126	66	1887	48	9984.8	54.9	19	999	3424	85.583
L	13	128	166	1918.3	51	212.76	55.18	19	1002	2210	1.384
M	6	91	98	1493.7	42	2665.8	54.77	17	997.5	3045	20.634
N	6	98	119	343.3	33	9971.2	55.31	18	1003.5	1479	36.451
O	11	110	157	198.3	42	9613.7	55.27	20	1003	1674	22.36
P	8	93	164	1898.7	36	9062.8	55.81	16	1009	2683	143.171
Q	15	133	195	574.1	51	343.27	55	17	1000	1849	1.714
Minimum	3	76	46	16.2	33	212.76	54.68	16	996.5	790	1.384
Maximum	21	164	302	1937.7	54	9997.6	56.8	46	1020	3552	143.171
Average	10.125	110.688	147.375	1215.1	42.813	6459.3	55.3206	20.4375	1003.6	2392.188	39.8079375

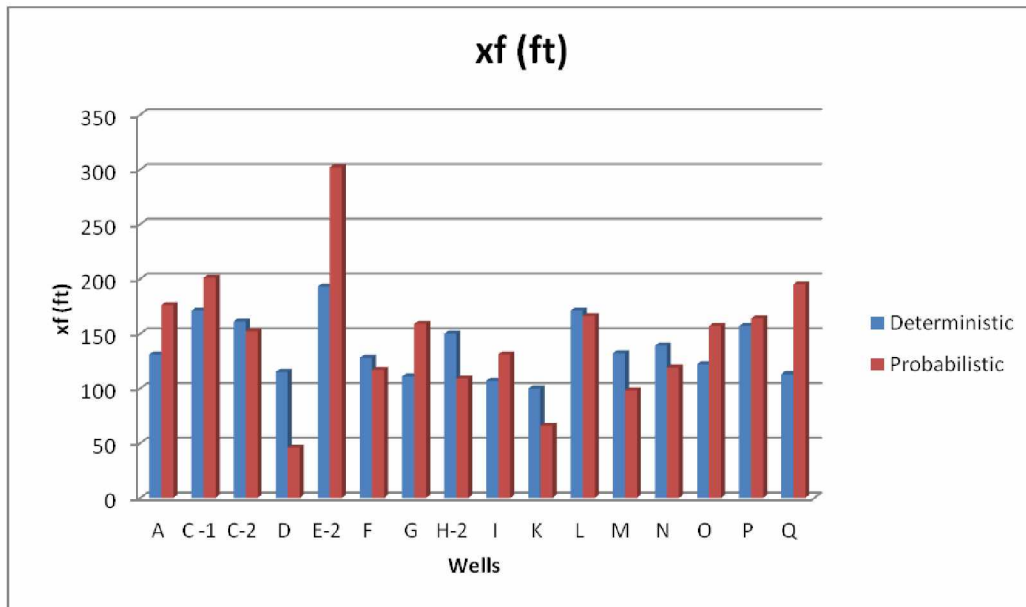


Figure 3.15 Fracture half-length values for each well using both approaches.

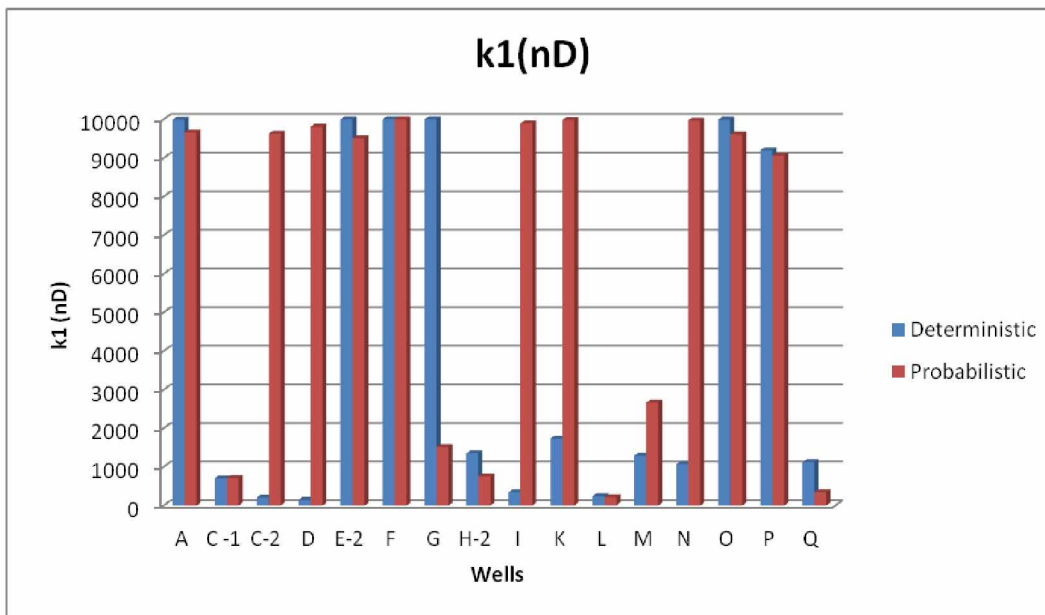


Figure 3.16 Bar chart for matrix permeability for both approaches.

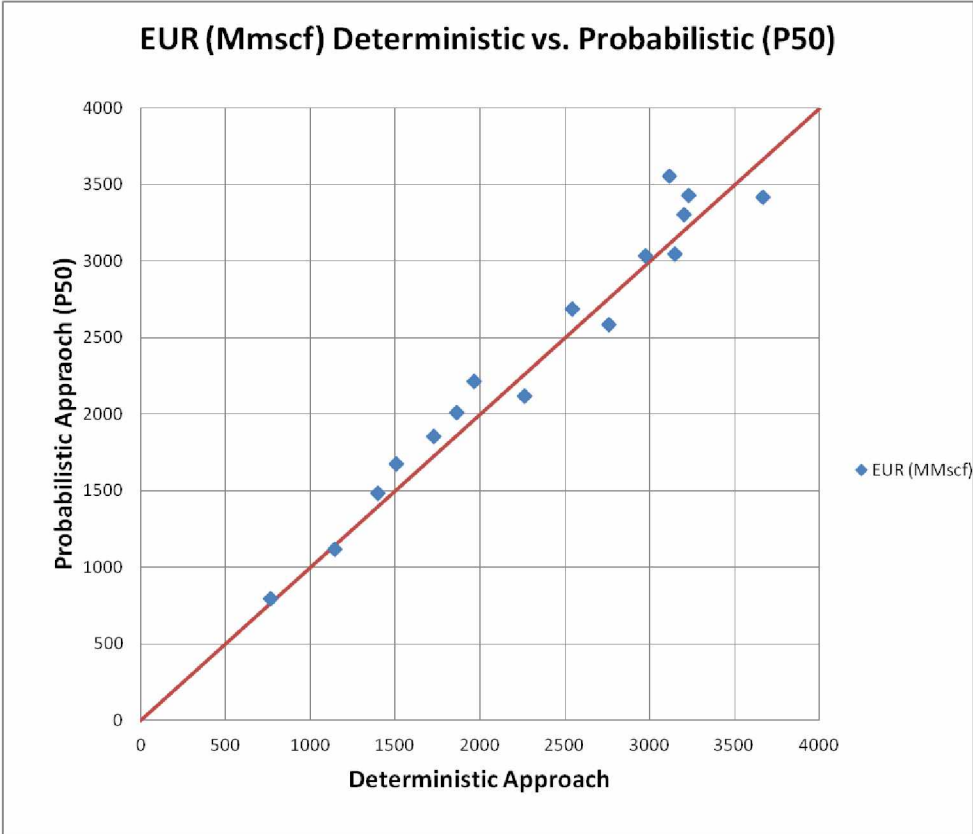


Figure 3.17 Deterministic vs. Probabilistic Approach EUR output.

CHAPTER 4 Part 2 - Completion Effectiveness & Performance Drivers

Achieving economical production from shale assets depends on the design of completion parameters. These parameters include the lateral length of the well, amount of proppant and liquid pumped, number of stages, cluster spacing, and the radius of the lateral wellbore. Discrete single well modeling is generally adopted as the traditional approach in evaluating completion effectiveness. The available response data in terms of production data is calibrated in the model and alternate completion scenarios are run to compare production profiles. These types of models are not ideal in the case of reservoirs like the Eagle Ford, which has complex geology and multiple reservoir fluid windows. The initial attempt was to conduct the analysis based on the existing database. EUR results from previous analysis were used to generate correlation with completion parameters. Since no strong correlation was established the total cumulative production (Gp) was used to conduct the analysis. Figure 4.1 shows plots between the design parameters and the total cumulative gas production. It is evident from these plots that no strong correlation exists between the observed production data and the different types of design parameters.

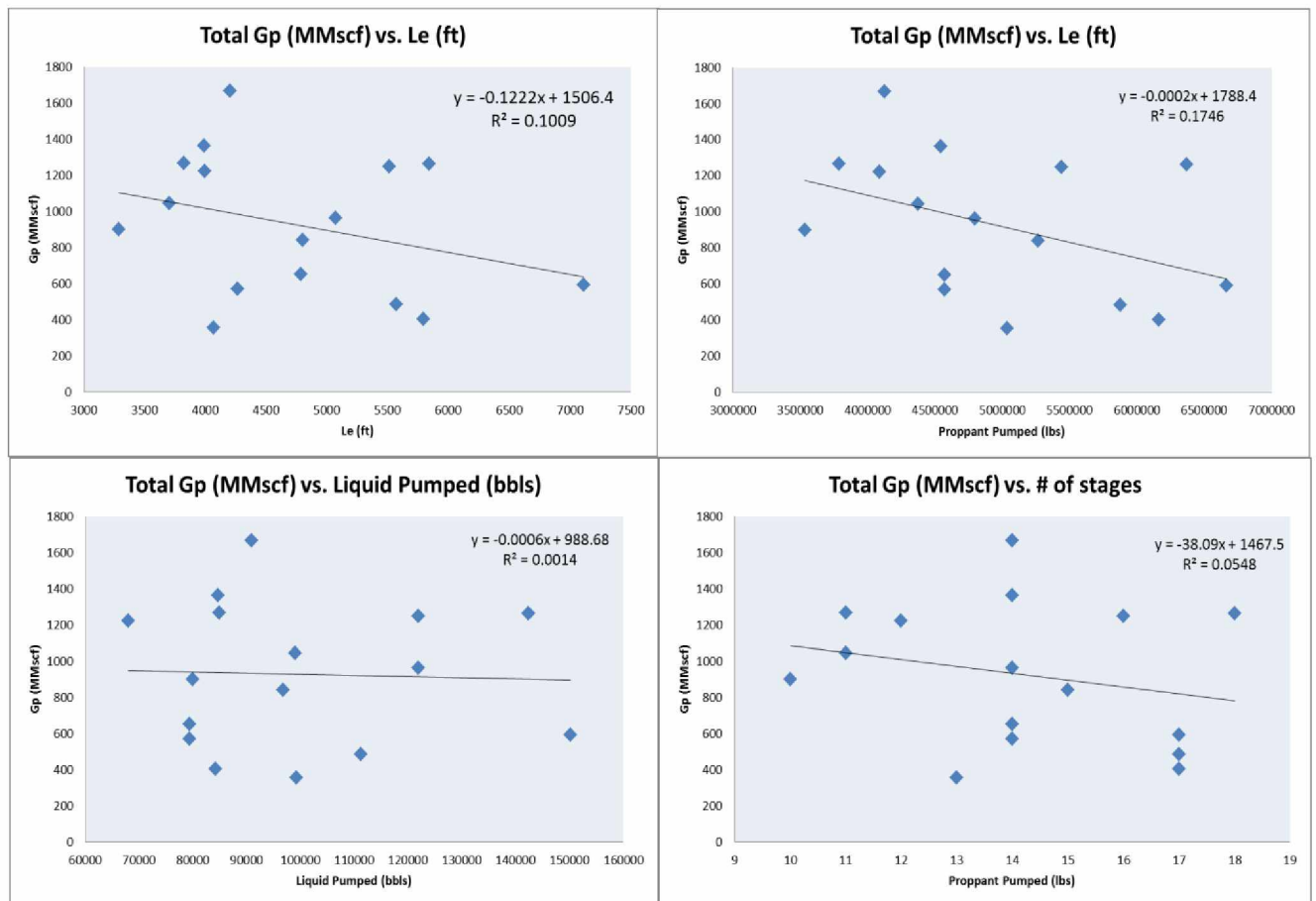


Figure 4.1 Plots for Total Gp vs. Design Parameters.

The total production for all the wells varies due to varying time periods. In order to have a valid comparison for all the wells, a common producing time for all the wells was necessary. The shortest amount of time produced by Well Q was 5 months. Hence, a 5 month cumulative gas production was selected for all the wells. Figure 4.2 is a 5 month production comparison to the design parameters. Once again it is evident that no strong relation was observed between 5 month cumulative production and design parameters.

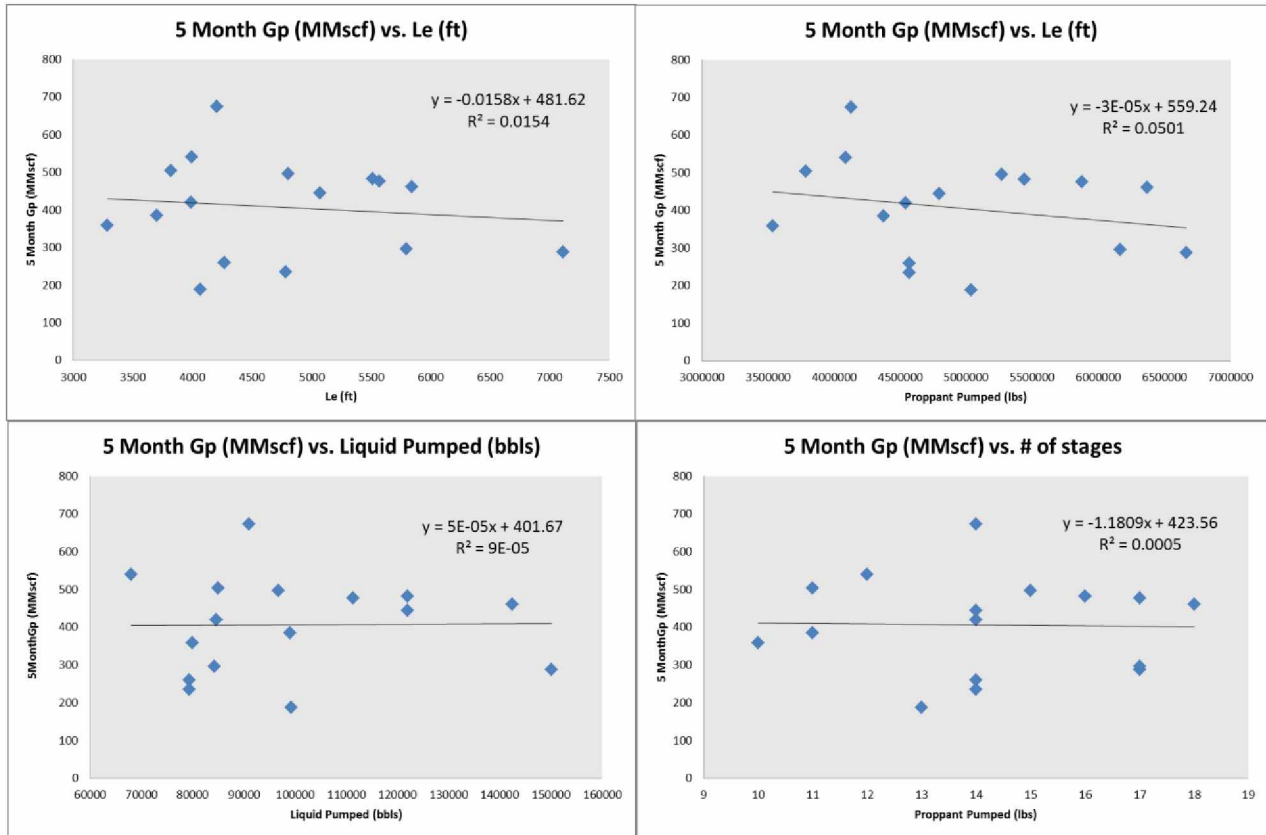


Figure 4.2 Comparison plots for 5 month cumulative production to different design parameters.

In order to evaluate the effect of completion on total production, a neural network model technique was adopted. Neural network modeling is based on analyzing the data in a system to find connections between the system input and output variables without explicit knowledge of the physical behavior of the system (Shelley et al., 2012). This approach was adopted because neural network modeling allows building models based on available data without prior assumptions or knowledge about the data. With this idea it was possible to identify the relationship between independent parameters (completion parameters) and dependent parameters (total production).

4.1 Artificial Neural Network

Neural network modeling is based on human brain function: it is biologically inspired computational modeling. Neural network models are developed by training the network to represent the relationships and processes that are inherent within the data (Nejad et al., 2015). Upon completion of the training to a certain satisfaction, generally the “R” value, the neural network models are put into operation. To test the validity of the model, new input data is passed through the trained neural network models to produce desired model outputs, which are compared with the actual outputs. Nejad and others (2015) suggest that the heuristic nature of neural network training can be addressed by using a genetic algorithm (GA) to train thousands of networks and choose the best network that has the least prediction error and satisfies engineering principles.

The fundamental building block for a neural network is the single-input neuron, such as the example shown in Figure 4.3.

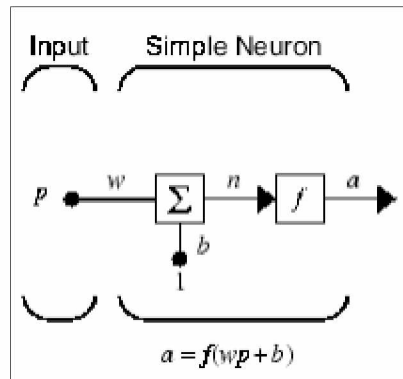


Figure 4.3 Single input neuron process. (MATLAB Neural Network Toolbox™. Version 8.2.1 User Guide).

The above figure can be broken down into three distinct functional operations. The scalar input p is multiplied by the scalar weight w to form the product wp , which is added to the scalar bias b to form the net input n (Matlab User Manual). The bias can be viewed as shifting the function f to the left by an amount b and a constant input of 1. Finally, the scalar output a is produced after the net input is passed through the transfer function f . The scalar parameters of the neuron w and b are both adjustable such that the network exhibits some interesting or desired behavior. By adjusting the weight or the bias parameter, the network can be trained to do a particular job.

4.1.1 Parameter Selection for Modeling

It is evident from the previous plots of cumulative production vs. design parameters that the relationship between different parameters and well production is unclear. For this reason, the Artificial Neural Network Modeling approach was adopted and models were trained based on the data provided by the operator for each well. The operator provided data for the following design parameters:

- Lateral Length (ft)
- Wellbore Radius (ft)
- Number of Stages
- Cluster Spacing (ft)
- Proppant Pumped (lbs)
- Liquid Pumped (lbs)
- Pump Rate (bbl/min)

The type of proppant pumped (20/40, 30/40 mesh size, etc.) and amount of fluid recovered (bbls.) after flowback were not considered in the analysis because these data were not available for all the wells. Out of the 16 wells used for this analysis, two wells showed high condensate production. This is captured in the location based per-well size chart shown in Figure 4.4. It is evident that wells in the southwest region are high condensate wells. This is possibly due to the fact they are closer to the condensate window. This introduced a non-controllable reservoir parameter to be considered within the analysis. Other non-controllable reservoir parameters that were considered in the analysis were:

- Initial Reservoir Pressure (psi)
- Pay Thickness (ft.)

The model was generated using inputs from the parameters discussed in the above section. Individual parameter data for each well was used as input and five month cumulative production was the output. This information was provided to the *Matlab* software through which the model generation process was conducted. Table 4.1 summarizes all the controllable and non-controllable parameters used for this analysis.

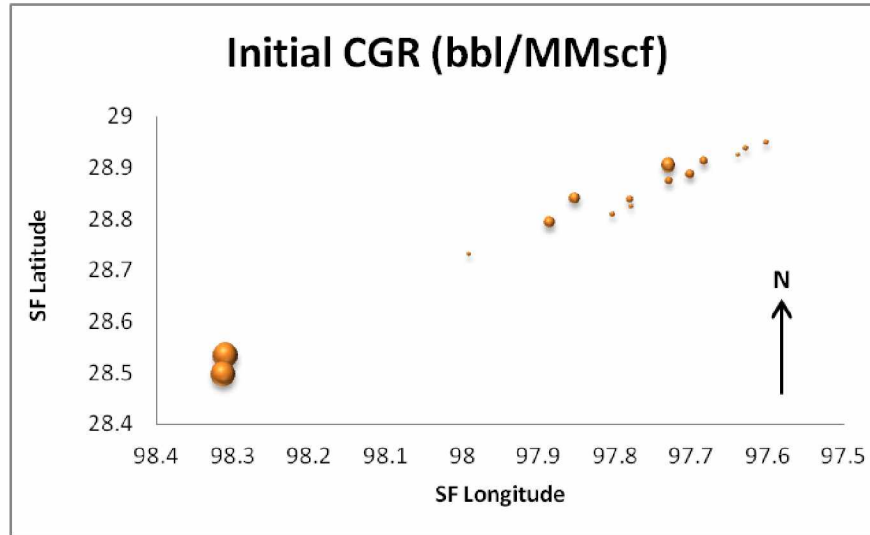


Figure 4.4 Initial condensate gas ratio for each well.

Table 4.1 Input Parameters for ANN modeling

Parameters	Type
Lateral Length - L_e (ft)	Controllable
Wellbore Radius - r_w (ft)	Controllable
No. of Stages	Controllable
Cluster Spacing - CS (ft)	Controllable
Proppant Pumped (lbs)	Controllable
Liquid Pumped (bbls)	Controllable
Pump Rate (bbl/min)	Controllable
Pay Thickness - h (ft)	Non-Controllable
CGR-Initial (bbl/MScf)	Non-Controllable
Pressure Gradient (psi /ft)	Non-Controllable

4.2 Artificial Neural Network Generated – 5 Month Production Model

An ANN model was prepared using MATLAB with the parameters mentioned in the above section. After training, since the input and output variables were known, the weights and biases of the hidden layer were used to prepare regression plots of the ANN model and observe its performance. The R value was used as a means of ascertaining whether or not the model was sufficiently accurate to predict the 5 month cumulative production. Figure 4.5 shows the results for the generated model. The prediction accuracy of the model is given by the R value of 0.99 ($R^2 = 0.98$). This is a significantly higher prediction capability of the model and was considered reasonable for this analysis. Figure 4.6 shows the plot for “Predicted vs. Actual values,” from which it is evident that most of the values lie close to the 45° line.

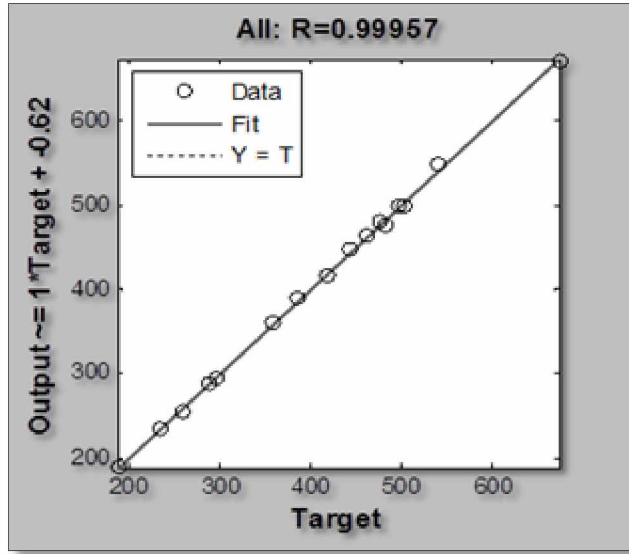


Figure 4.5 ANN Model Regression Plot.

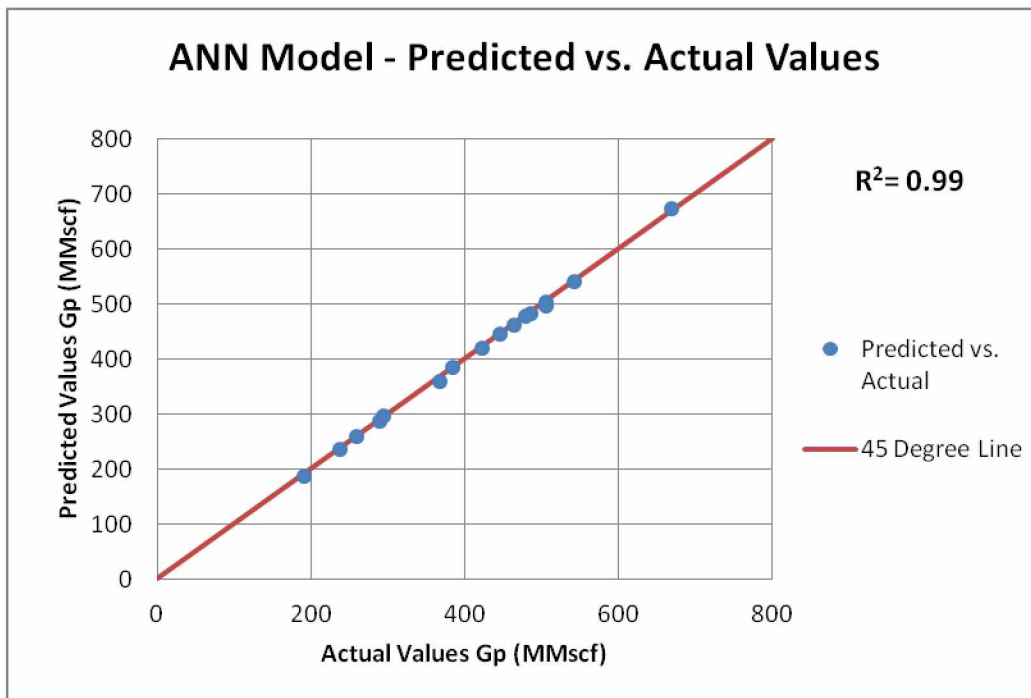


Figure 4.6 ANN Model Predicted vs. Actual Values.

4.3 Parameter Sensitivity

An initial analysis on parameter sensitivity to cumulative production was conducted. This was done by holding all the parameters constant and changing one parameter at a time. A change of +10% was applied

to each individual parameter range. Figure 4.7 shows a bar chart with the parameters having highest sensitivity to the cumulative production. It is evident from this chart that uncontrollable parameters like reservoir pressure and condensate gas ratio are the most sensitive to cumulative production. Cluster Spacing and Proppant Pumped were amongst the most sensitive design parameters, followed by Number of Stages and Liquid Pumped.

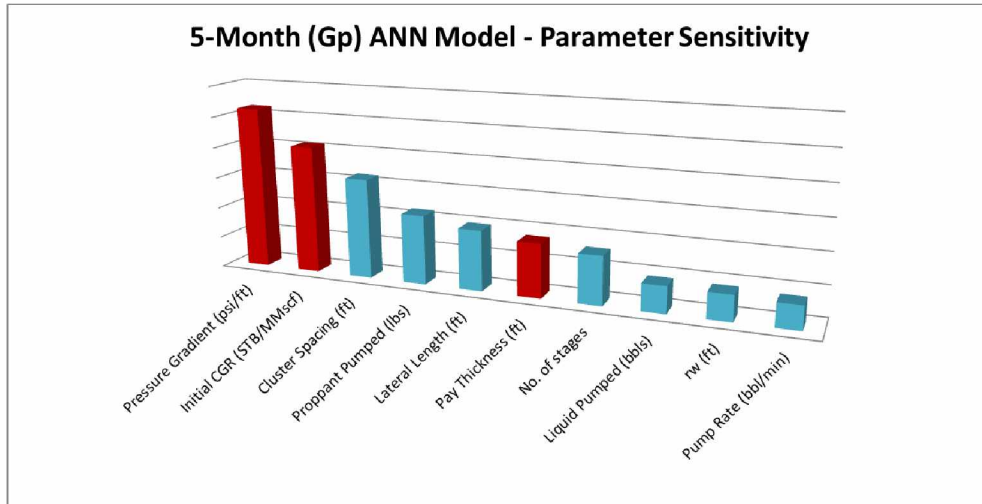


Figure 4.7 Bar Chart for 5 Month Production Model – Parameter Sensitivity Completion Effectiveness.

Using the information learned from the parameter sensitivity study, an analysis was conducted to test if the wells were over-stimulated or under-stimulated. Based on the sensitivity of the design parameters, this analysis was conducted by varying the following parameters:

- Cluster Spacing (ft)
- Proppant Pumped (lbs)
- Number of Stages
- Lateral Length

Each parameter was increased by 10% of its original range while keeping the other parameters constant for all the wells. This was done to see the individual effect on cumulative production for each well. Any significant change in the 5 month cumulative production was noted. Figure 4.8 shows results for the varied parameters. Increasing Cluster Spacing increased the cumulative production significantly, which was observed for almost all the wells. Increasing the amount of Proppant Pumped showed an opposite trend, where most wells showed a decrease of as much as 70%. Increasing number of stages for each well did not have a significant change except for Well C-2 and Well Q. Increasing the Lateral-length parameter significantly increased the cumulative production for all wells, which was an expected result

since increasing the exposure to total stimulated area will evidently increase the production. Table 4.2 summarizes the results for all the wells. From this analysis it was evident that Well C-2 and Well K were both over-stimulated and under-stimulated. These wells were chosen as candidates for the completion optimization study.

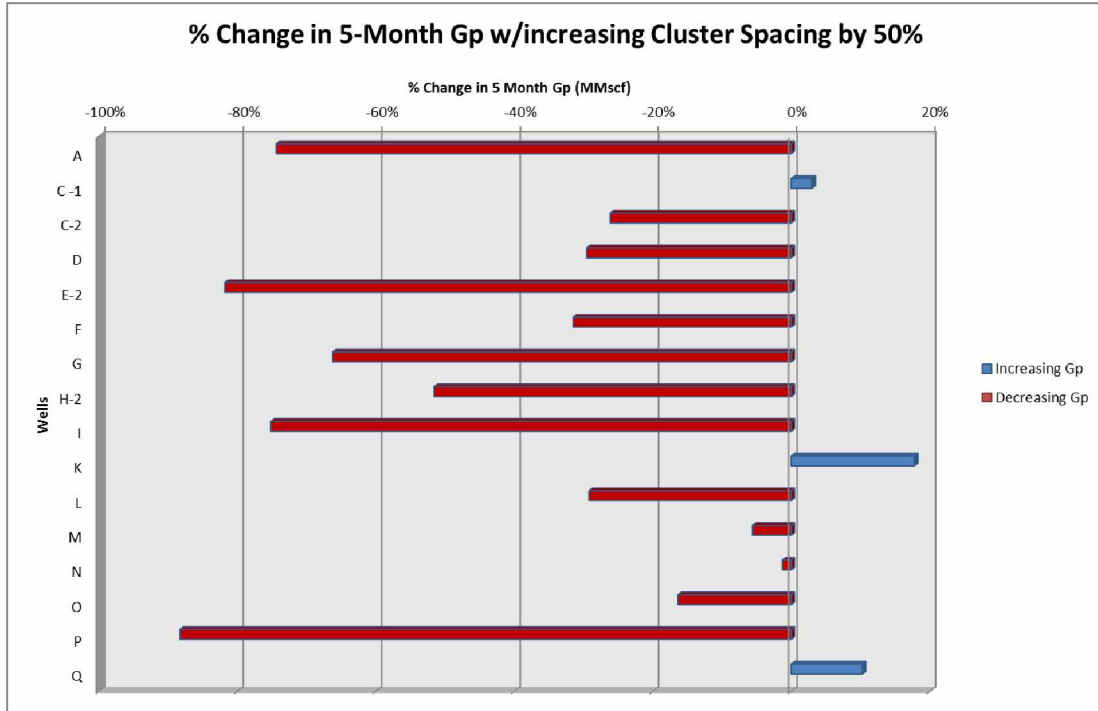


Figure 4.8 Bar chart for change in cluster spacing by 50%.

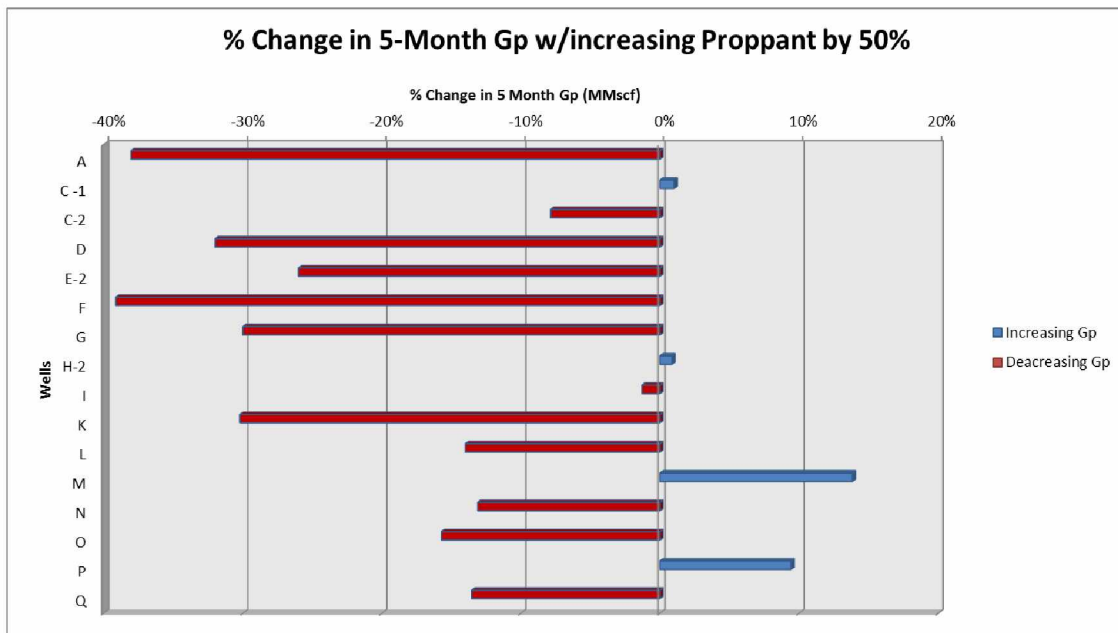


Figure 4.9 Bar chart for amount of Proppant pumped by 50%.

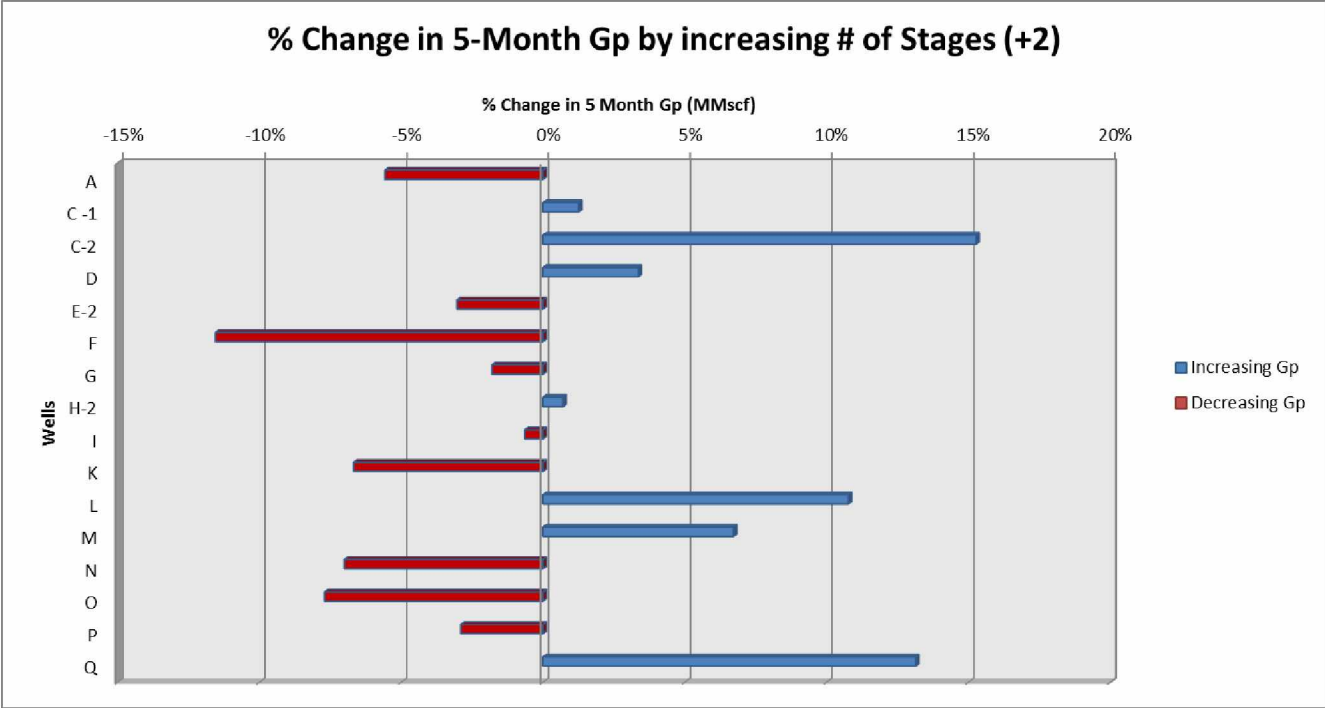


Figure 4.10 Bar chart for change in number of stages.

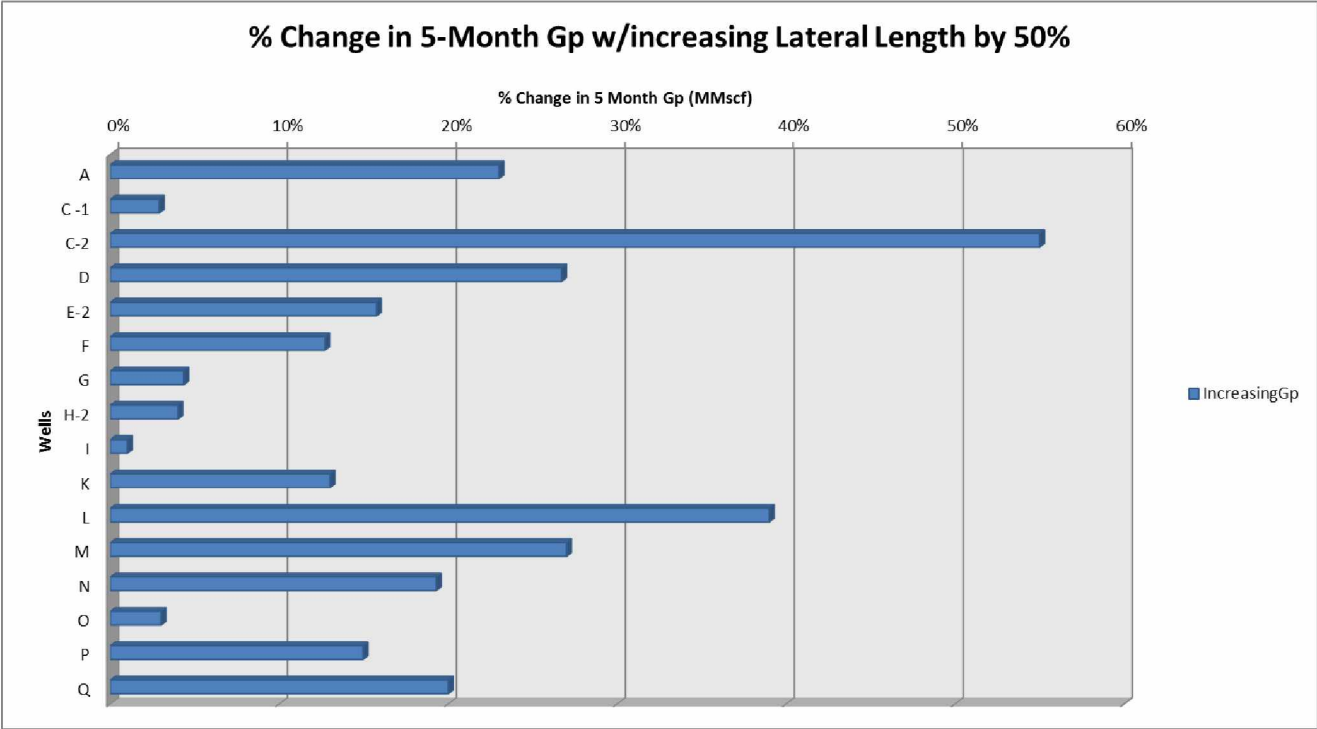


Figure 4.11 Bar chart for change in length of Lateral Length

Table 4.2 Summary of all the varied parameters for each well

Wells	Cluster Spacing (ft)	Proppant Pumped (lbs)	Lateral Length (ft)	No. Of Stages
A	Understimulated	Not Significant	Understimulated	Overstimulated
C -1	Overstimulated	Not Significant	Understimulated	Not Significant
C-2	Understimulated	Overstimulated	Understimulated	Understimulated
D	Understimulated	Overstimulated	Understimulated	Not Significant
E-2	Understimulated	Not Significant	Understimulated	Not Significant
F	Understimulated	Not Significant	Understimulated	Overstimulated
G	Understimulated	Overstimulated	Understimulated	Not Significant
H-2	Understimulated	Not Significant	Understimulated	Not Significant
I	Understimulated	Not Significant	Understimulated	Not Significant
K	Overstimulated	Overstimulated	Understimulated	Overstimulated
L	Understimulated	Understimulated	Understimulated	Not Significant
M	Overstimulated	Understimulated	Understimulated	Not Significant
N	Overstimulated	Not Significant	Understimulated	Overstimulated
O	Overstimulated	Not Significant	Understimulated	Overstimulated
P	Understimulated	Not Significant	Understimulated	Not Significant
Q	Overstimulated	Not Significant	Understimulated	Understimulated

4.4 Completion Scenarios

The previous analysis helped to identify candidate wells for the completion optimization study. The existing ANN model was used to predict 5 month cumulative production by changing the parameters of interest. Well C-2 is located in the southwest part of the reservoir and has a lower 5 month total production of 187.9 (MMscf) and a high initial condensate to gas ratio of 361 (bbl/Mscf). Well K is located in the northeast region of the reservoir and has a higher 5 month cumulative gas production of 482.69 (MMscf) and low initial condensate to gas ratio of 60 (bbl/MMscf). The two wells were completed in a similar manner, with the major difference between them being their location within the reservoir. Different completion and fracturing scenarios were considered to evaluate individual well potential and provide direction to improve production for future wells. Four different scenarios were considered to evaluate their effect on the 5 month cumulative gas production. The selection of these scenarios was based on the observations made in the parameter sensitivity study. The model sensitivity indicated that controllable design parameters like cluster spacing, frac stages, and proppant and liquid pumped were most sensitive to production. The parameters were varied for this analysis using different scenarios:

- **Scenario 1:** The number of frac stages and amount of proppant pumped was increased by a factor of 0.5 while keeping other parameters constant.
- **Scenario 2:** The number of frac stages and lateral length were increased by a factor of 0.5 while keeping other parameters constant to their original value.
- **Scenario 3:** The number of lateral length and proppant pumped was increased by a factor of 0.5 while keeping other parameters constant.
- **Scenario 4:** The cluster spacing was decreased by a factor of 0.5 while keeping other parameters constant.

The results from the analysis are summarized in Figures 4.12 and 4.13. The 5 month gas cumulative of 189.79 (MMscf) is estimated by the ANN model to be over predicted by 1%. This is reflected in the second column of the bar chart of Figure 4.12. The operator stimulated this well in 13 stages using over 5 MM lbs of sand and 95 M (bbls) of liquid, pumped at an average rate of 60 BPM. For Scenario 1, the number of fracture stages was increased to 20, which showed an increase in 5 month production by 2.38%. In Scenario 2, the number of fracture stages was increased along with the amount of proppant pumped. Scenario 2 showed an increase of 3.97% in the 5 month cumulative gas production. Scenario 3 did not show any significant increases as compared to Scenario 1 & 2 in cumulative production when lateral length and proppant pumped were increased. Scenario 4 was the best design scenario for Well C-2 when cluster spacing of 30 ft was considered in the completion, since cumulative production increased significantly, to 19.84%. This scenario might be the best economic option since other parameters are kept constant and only closer cluster spacing is decreased i.e. closer fracture spacing. More studies regarding fracture shadowing and fracture interference should be conducted to confirm the optimal cluster spacing. Table 4.3 summarizes all the scenario results for Well C-2.

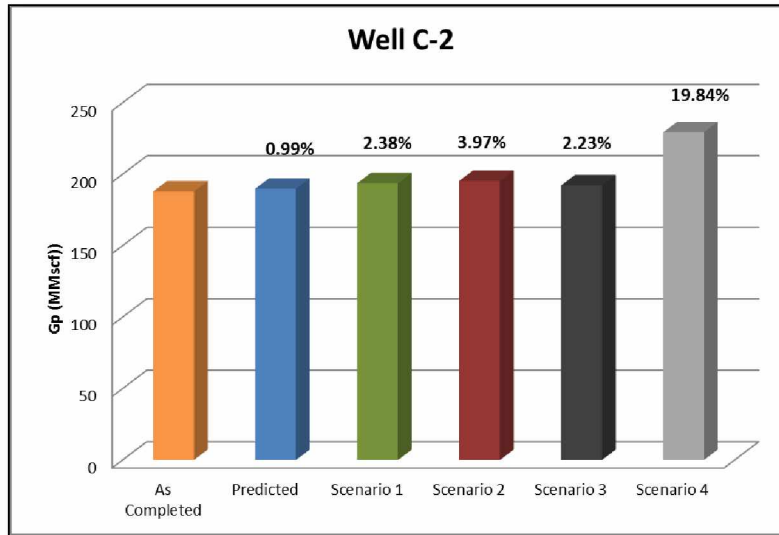


Figure 4.12 Bar chart for Well C-2 completion optimization results.

Table 4.3 Scenario Results Summary for Well C-2

Parameters	Model Predicted	Scenario 1	Scenario 2	Scenario 3	Scenario 4
Cluster Spacing (ft)	62.62	62.62	62.62	62.62	31.31
Proppant Pumped (lbs)	5037320	7555980	5037320	7555980	5037320
Lateral Length (ft)	4070	4070	6105	6105	4070
# of Stages)	13	20	20	13	13
5 month Gp (MMscf)	189.7966	193.684	195.29	224.524	229.3037
% Change	0.99%	2.38%	3.97%	2.24%	19.84%

Well K was completed by the operator with 16 stages and used over 5 MM (lbs) of proppant and with a lateral length of 4070 ft. Results are summarized in Figure 4.13. In Scenario 1, the number of fracture stages was increased to 24 along with proppant pumped to 8.16 MM lbs., which showed a decrease in 5 month production of 16.5%. In Scenario 2, the number of fracture stages was increased along with the length of lateral to 6105 ft. and the model predicted an increase of 21.5% for the 5 month cumulative gas production. For Scenario 3, a lesser decrease in cumulative production was observed compared to that of

Scenario 1. This may suggest that increasing designing parameters like fracture stages, proppant, and lateral length will in fact decrease the cumulative production due to overstimulation. Similar to Well C-2, Scenario 4 was also one of the best design scenario for Well K, when cluster spacing of 30 ft was considered in the completion: the 5 month cumulative production increased by 16.1%. This may suggest that closer fracture spacing will yield higher production since a greater reservoir area will have enhanced permeability. In the case of long term production, fracture-shadowing and fracture-interference studies should be conducted to select the optimum fracture spacing. Table 4.4 summarizes all the scenario results for Well K.

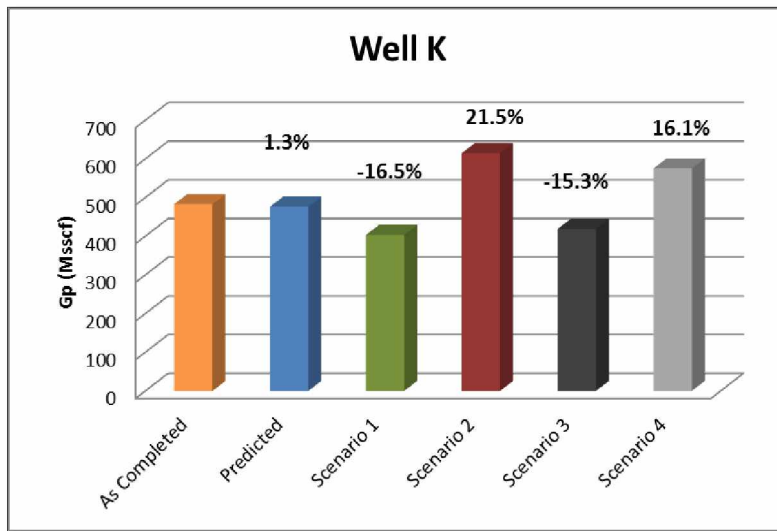


Figure 4.13 Bar chart for Well K completion optimization.

Table 4.4 Scenario Results for Well K

Parameters	Model Predicted	Scenario 1	Scenario 2	Scenario 3	Scenario 4
Cluster Spacing (ft)	68.94	68.94	68.94	68.94	34.47
Proppant Pumped (lbs)	5440325	8160487.5	5440325	8160487.5	5440325
Lateral Length (ft)	5515.00	5515.00	8272.50	8272.50	5515.00
# of Stages)	16	24	24	16	16
5 month Gp (MMscf)	476.2549	403.16	614.76	418.76	575.22
% Change	1.33%	-16.48%	21.48%	-15.27%	16.09%

CHAPTER 5 Conclusions and Recommendations

In the Part 1 of this study an integrated Rate Transient Analysis approach was introduced. Based on the data provided by the operator, a total of 16 of 21 gas wells in the Eagle Ford shale were analyzed. The analysis was conducted using two approaches: deterministic and probabilistic. This was done to address the uncertainty observed in evaluating well performance from shale gas wells, as discussed by Wattenbarger and others (1998). The deterministic approach adopted an Enhanced Fracture Region Model developed by Stalgorova and Mattar (2012). The commercial software used in this analysis incorporated this model, which was modified accordingly to evaluate shale gas wells. A 30-year forecast was generated using the deterministic approach and compared to the probabilistic P50 forecast. If the values were within an acceptable range (>15%), the analysis was considered completed. The analysis of the results from this study indicates the following conclusions:

- Due to the vast amount of variables and assumptions required, the analysis of production data from unconventional reservoir wells (shale gas wells, in this case) generates uncertainty in the results.
- The square-root time plot overestimated the A_{SRV} (acres) but the derived fracture half-length (x_f) was within a reasonable range when compared to the probabilistic results. The deterministic approach might not be the best method to estimate reservoir parameters such k_1 , k_2 , F_{CD} , and X_L , since many non-unique solutions can satisfy the same pressure history match.
- The number of fractures was estimated based on the most-likely approach proposed by Anderson and Liang (2011). This method defined a “parameter-space” consisting of allowable combinations of total fracture area and drainage area and used a P50 value for number of fractures based on the bulk well performance parameter.
- Both the deterministic and probabilistic approaches gave reliable results in terms of 30-year EUR forecasts. All EUR results were within the acceptable threshold value range of 15%. Figure (??) compares the deterministic and probabilistic EUR results. It is evident from this plot that for most wells the values are fairly close to the forty-five degree line.
- The deterministic model is not sufficient to estimate physical reservoir parameters. The probabilistic approach provided reliable estimates for fracture half-lengths (x_f), stimulated reservoir permeability (k_1), and matrix permeability (k_2), but other parameters, such as fracture conductivity (F_{CD}) and stimulated reservoir area volume (A_{SRV}), had systematic errors.
- If production forecasting is the sole requirement for an analysis, the suggested workflow provides a consistent approach in conducting Rate Transient Analysis on shale gas wells.

Part 2 of this study consisted of developing an Artificial Neural Network model to evaluate completion efficiency and identify design parameter effectiveness on the wells analyzed in Part 1. The Artificial Neural Network model was trained using MATLAB software on the database comprising 16 shale gas wells. The genetic algorithm used in developing the model evaluated various combinations of input parameters and generated an appropriate neural network topology. The model validation was carried out by comparing the predicted values to the actual values. Figure 4.6 shows the accuracy of the model with a R^2 value of 0.99 and the “Predicted vs. Actual Model” data points lying on the forty-five degree line. The following are the results and observation made while conducting this analysis:

- The parameter sensitivity analysis showed that uncontrollable reservoir parameters like pressure gradient and condensate to gas ratio are the most influential parameters on cumulative recovery. This suggests that hydrocarbon thermal maturity may dominate the gas production in the Eagle Ford shale.
- Modeling of this database showed that cluster spacing, proppant pumped, number of stages, and liquid pumped were among the most influential design parameters on cumulative gas production. It was surprising to observe that lateral length and wellbore radius did not influence cumulative production. Since most wells had an average lateral length of 4500 ft, any increase or decrease in the parameter would not necessarily improve production.
- The completion effectiveness study showed that 8 out of 16 wells were either under-stimulated or over-stimulated. This information is useful to the operator and can be used to design future wells within the region.
- Wells C-2 and K were used as subject wells to conduct the completion optimization study. It was found that decreasing cluster spacing to 30 ft for both the wells will significantly improve the 5-month cumulative production. It is suggested that this figure be supported with results from fracture interference and fracture shadowing studies.
- Increasing the amount of proppant and liquid pumped and the number of stages improved the production of Well C-2 significantly. This well is a high condensate well and close to the condensate window. Increasing proppant and liquid volumes is suggested, but completion design economics should be conducted to consider this option. Well K showed a decrease in cumulative production upon increasing proppant and liquid volumes. This may suggest that wells in the northeast gas window do not need high volumes of proppant and liquid, but rather closer cluster spacing.
- The ANN model is a good tool to evaluate the effectiveness of completion on cumulative production. It is recommended that economic analyses be conducted to support these results.

CHAPTER 6 Appendix

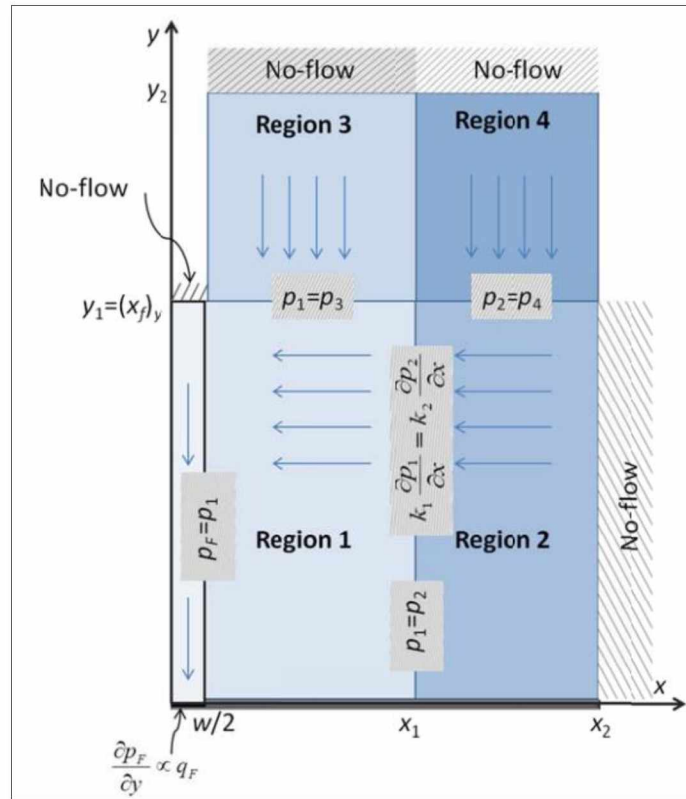


Figure 6.1 Flow directions and boundary conditions for the Five-Region Model (Stalgorova and Mattar, 2012).

Each region is governed by the following diffusivity equation:

$$\nabla^2 p = \frac{\phi \mu c}{k} * \frac{\partial p}{\partial t}$$

The authors re-write the above equation in dimensionless terms for each region and convert it to Laplace domain. Starting with the outermost region, derivation of the above equation for each region described by Stalgorova and Mattar (2012) is as follows.

Region 4:

Diffusivity equation becomes: $\frac{\partial^2 p_{avg_{4D}}}{\partial y_D^2} - \frac{s}{\eta_{4D}} p_{avg_{4D}} = 0$

where $p_{avg_{4D}}$ is the pressure in region 4 in Laplace domain.

Boundary condition 1: no-flow at the outer reservoir boundary ($y=y_2$)

$$\left(\frac{\delta p_{avg_{4D}}}{\delta y_D} \right)_{(y_D=y_{2D})} = 0$$

Boundary condition 2: pressure continuity between regions 4 and 2 (at $y = y_1$)

$$p_{avg_{4D}}(y_{1D}) = p_{avg_{2D}}(y_{1D})$$

Region 3:

Diffusivity equation becomes:

$$\frac{\partial^2 p_{avg_{3D}}}{\partial y_D^2} - \frac{s}{\eta_{3D}} p_{avg_{3D}} = 0$$

where $p_{avg_{3D}}$ is the pressure in region 3 in Laplace domain.

Boundary condition 1: no-flow at the outer reservoir boundary ($y=y_2$)

$$\left(\frac{\delta p_{avg_{3D}}}{\delta y_D} \right)_{(y_D=y_{2D})} = 0$$

Boundary condition 2: pressure continuity between regions 3 and 1 (at $y = y_1$)

$$p_{avg_{3D}}(y_{1D}) = p_{avg_{1D}}(y_{1D})$$

Region 2:

Diffusivity equation becomes:

$$\left(\frac{\partial^2 p_{avg_{2D}}}{\partial x_D^2} + \frac{k_4}{k_2 y_{1D}} * \frac{\partial p_{4D}}{\partial y_D} \right)_{y_{1D}} - \frac{s}{\eta_{3D}} p_{avg_{2D}} = 0$$

where $p_{avg_{2D}}$ is the pressure in region 3 in Laplace domain.

Boundary condition 1: no-flow midway between the fractures

$$\left(\frac{\delta p_{avg_{2D}}}{\delta x_D} \right)_{(x_{2D})} = 0$$

Boundary condition 2: pressure continuity between regions 3 and 1 (at $y = y_1$)

$$p_{avg_{2D}}(x_{1D}) = p_{avg_{1D}}(x_{1D})$$

Region 1:

Diffusivity equation becomes:

$$\left(\frac{\partial^2 p_{avg_{1D}}}{\partial x_D^2} + \frac{k_3}{k_1 y_{1D}} * \frac{\partial p_{3D}}{\partial y_D} \right)_{y_{1D}} - \frac{s}{\eta_{1D}} p_{avg_{1D}} = 0$$

where $p_{avg_{2D}}$ is the pressure in region 3 in Laplace domain.

Boundary condition 1: flux continuity between regions 2 and 1

$$\left(\frac{k_2}{\mu} \right) \left(\frac{\delta p_{avg_{2D}}}{\delta x_D} \right)_{(x_{1D})} = \left(\frac{k_1}{\mu} \right) \left(\frac{\delta p_{avg_{1D}}}{\delta x_D} \right)_{(x_{1D})}$$

Boundary condition 2: pressure continuity between regions 1 and Fracture region

$$p_{avg_{1D}}(w_D/2) = p_{avg_{FD}}(w_D/2)$$

Fracture Region:

Diffusivity equation becomes:

$$\left(\frac{\partial^2 p_{avg_{FD}}}{\partial y_D^2} + \frac{2}{F_{CD}} * \frac{\partial p_{1D}}{\partial x_D} \right)_{w_D/2} - \frac{s}{\eta_{FD}} p_{avg_{FD}} = 0$$

where $p_{avg_{2D}}$ is the pressure in region 3 in Laplace domain.

Boundary condition 1: no flow through the fracture tip ($y_D = y_{1D}$)

$$\left(\frac{\delta p_{avg_{FD}}}{\delta y_D} \right)_{(y_{1D})} = 0$$

Boundary condition 2: applying Darcy Law at the wellbore ($y_D=0$)

$$\frac{\partial p_{avg_{FD}}}{\partial y_D} = - \frac{\pi}{F_{CD} * s}$$

Since the model applies to horizontal wells, a correction to account for flow line convergence in the fracture was introduced.

$$p_{avg_{wD}} = \frac{\pi}{F_{CD} * s * \sqrt{c_6(s) \tanh * (\sqrt{c_6(s)})}} + \frac{s_c}{s}$$

where s_c is the skin due to convergence, which can be calculated from:

$$s_c = \frac{k_1 h}{k_f w} \left[\ln \left(\frac{h}{2r_w} \right) - \frac{\pi}{2} \right]$$

This model was initially derived for a liquid system, but Stalgorova and Mattar (2012) proposed that real-gas pseudopressure should be used for dimensionless pressure. The commercial software used for this analysis adopts this model and makes the required corrections for the appropriate fluid type and reservoir.

CHAPTER 7 Nomenclature

A_c = Total fracture area, ft²

A_d = Drainage Area, ft²

c_t = Total compressibility, psi⁻¹

FCD' = Apparent fracture conductivity, dimensionless

EUR = Estimated Ultimate Recovery, bcf

h = Fracture height, h.

k_1 = matrix permeability, nD

k_2/k_{SRV} = stimulated reservoir volume permeability, nD

L = Horizontal well length, ft.

n_f = Number of fractures

OGIP = Original Gas in Place, bcf

P_i = Initial Reservoir Pressure, psia

P_p = Pseudo Pressure, psia

P_{wf} = Well bottom hole flowing pressure, psi

q = Gas Rate, MMscfD

t = Time, day

t_a = Pseudo time, day

T = Reservoir Temperature, °F

x_f = Fracture half-length, ft.

X_L = Enhanced permeability region distance from fracture tip, ft.

Z = Compressibility factor, dimensionless

ϕ = Porosity

μ = Viscosity, cP

CHAPTER 8 References

- Anderson, D.M. & Liang, P. 2011. Quantifying Uncertainty in Rate Transient Analysis for Unconventional Gas Reservoirs. Paper SPE 145088 presented at the SPE North American Unconventional Gas Conference and Exhibition. The Woodlands, TX. 14-16 June. <http://dx.doi.org/10.2118/145088-MS>
- Anderson, D.M. Nobakht, M. Moghadam, S. Mattar, L. 2010. Analysis of Production Data from Fractured Shale Gas Well. Paper SPE 131787 presented at the SPE Unconventional Gas Conference, Pittsburgh Pennsylvania. 23 - 25 February. <http://dx.doi.org/10.2118/131787-MS>
- Anderson, D.M. Thompson, J.M. 2014. How Reliable Is Production Data Analysis? Paper SPE 169013 presented at the Unconventional Resources Conference. The Woodlands, TX. 1 – 3 April. <http://dx.doi.org/10.2118/169013-MS>
- Beard, T. 2011. Fracture Design in Horizontal Shale Wells-Data Gathering to Implementation. US Environmental Protection Agency. EPA Hydraulic Fracturing Workshop. March 10 -11th, 2011.
- Bukola K. O. and Aguilera R. 2014. Multi-stage Hydraulic Fracturing Design in Horizontal Wells with the Use of Drill Cuttings. Paper SPE 169572 presented at the SPE Western North American and Rocky Mountain Joint Regional Meeting, Denver, Colorado, 16-18 April. <http://dx.doi.org/10.2118/169572-MS>
- Daneshy, A. A. 2003. Off-Balance Growth: A New Concept in Hydraulic Fracturing Journal of Petroleum Technology 55(4): 78-85. SPE 80992-MS. <http://dx.doi.org/10.2118/80992-MS>
- "Eagle Ford Shale Geology." *The Eagle Ford Shale Main*. N.p., n.d. Web. 06 July 2014. <<http://eaglefordshale.com/geology/>>.
- EIA. 2011. Review of Emerging Resources: U.S. Shale Gas and Shale Oil Plays, <http://www.eia.gov/analysis/studies/usshalegas.html> (accessed July 7, 2014).
- Geertsma, J. and de Klerk, F. 1969 A Rapid Method of Predicting Width and Extent of Hydraulically Induced Fractures. In Transactions of the Society of Petroleum Engineers, Vol. 246, Part 12, 1571-1581. Richardson, Texas: Society of Petroleum Engineers, ISBN 0149-2136.
- Gidley, J. L. Holditch S. A. Nierode, D. E. and Veatch, R. W. 1989. Recent Advances in Hydraulic Fracturing. Monograph Volume 12. 39-241. Richardson, Texas, SPE.
- Irwin, G. (1957): "Analysis of Stresses and Strains near the End of a Crack". Journal of Applied Mechanics, 24, pp. 361.
- Jackson, J.A. (1997). Glossary of Geology, 4th Ed. American Geological Institute.
- Kennedy, R. et al. 2012. Optimized Shale Resources Development: Proper Placement of Wells and Hydraulic Fracture Stages. Paper SPE-162534 prepared for presentation at the Abu Dhabi International Petroleum Conference and Exhibition held in Abu Dhabi, UAE, 11-14 November. <http://dx.doi.org/10.2118/162534-MS>

- Martin, R. Baihly, J. Malpani, et Al. 2011. Understanding Production from Eagle Ford – Austin Chalk System. Paper SPE 145117 presented at the Annual technical Conference and Exhibition held in Denver, Colorado, 30 October – 2 November. <http://dx.doi.org/10.2118/145117-MS>
- Martinez, David. 2012. Fundamental Hydraulic Fracturing Concepts for Poorly Consolidated Formations. PhD dissertation, University of Oklahoma, Norman, Oklahoma (August, 2012).
- Masters, J.A. (1979). Deep Basin Gas Trap, Western Canada. AAPG Bulletin 63, No. 2, 152.
- MATLAB Neural Network Toolbox™. Version 8.2.1 User Guide. 2014. Natick, MA: MATLAB.
- Mattar L. & Anderson, D.M. 2003. A Systematic and Comprehensive Methodology for Advanced Analysis of Production Data. Paper SPE 84472 presented at the SPE Annual Technical Conference and Exhibition. Denver, Colorado. 5 – 8 October. <http://dx.doi.org/10.2118/84472-MS>
- Mayerhofer, M.J. Lolon, E.P. et. Al. 2008. What is Stimulated Reservoir Volume (SRV)? Paper SPE 119890 presented at the SPE Shale Gas Production Conference, Fort Worth, Texas. 16-18 November. <http://dx.doi.org/10.2118/119890-PA>
- Mullen, J. 2010. Petrophysical Characterization of the Eagle Ford Shale in South Texas. Paper SPE 138145 presented at the Canadian Unconventional Resources & International Petroleum Conference. Calgary, Canada. 19-21 October. <http://dx.doi.org/10.2118/138145-MS>
- Nejad, A. M. Sheludko, S. Shelley, R. F. et Al. 2015. A Case History: Evaluating Well Completions in the Eagle Ford Shale Using a Data-Driven Approach. Paper SPE 173336 presented at the SPE Hydraulic Fracturing Technology Conference. The Woodlands, TX. 3 – 5 February.
- Nordgren, R.P. 1970. Propagation of a Vertical Hydraulic Fracture. Paper SPE 3009 presented at the SPE 45th Annual Fall Meeting, held in Houston, Texas, Oct. 4-7. <http://dx.doi.org/10.2118/3009-PA>.
- Orowan, E. (1952): “Fundamentals of Brittle Behavior in Metals”. W.M> Murray, Editor, Fatigue and Fracture of Metals, pp. 139-154. John Wiley, New-York, NY(USA).
- Ozkan, E. Brown, M., Raghavan, R. and Kazemi, H. 2009. Comparison of Fractured Horizontal-Well Performance in Conventional and Unconventional Reservoirs. Paper SPE 121290 presented at the SPE Western Regional Meeting, San Jose, California, 24-26 March. <http://dx.doi.org/10.2118/121290-MS>
- Palisch, T.T. Vincent, M.C. and Handren, P.J. 2008. Slickwater Fracturing-Food for Thought. Paper SPE 115766 presented at the SPE Annual Technical Conference and Exhibition held in Denver, Colorado, 21-24, September. <http://dx.doi.org/10.2118/115766-MS>
- Perkins, T.K. Kern, L.R. 1961. Widths of Hydraulic Fractures. Paper SPE 89 presented at the 36th Annual Fall Meeting of SPE held in Dallas, Texas, Oct. 8-11. <http://dx.doi.org/10.2118/89-PA>.
- Portis, D.H. Bello, H. Murray, M. et Al. 2013. Searching for the Optimal Well Spacing in the Eagle Ford Shale: A Practical Tool Kit. Paper SPE 168810 presented at the Unconventional Resources Technology Conference. Denver, CO. 12-14 August. <http://dx.doi.org/10.1190/URTEC2013-027>

Potluri, N.K. Zhu, D. and Hill D. 2005. The Effect of Natural Fractures on Hydraulic Fracture Propagation. Paper SPE 94568 presented at the SPE European Formation Damage Conference held in Sheveningen, The Netherlands, 25-27 May. <http://dx.doi.org/10.2118/94568-MS>.

Stalgorova, E. and Matter, L. 2012. Analytical Model for History Matching and Forecasting Production in Multifrac Composite System. Paper SPE 162516 presented at the SPE Canadian Unconventional Resources Conference. Calgary, Canada. 30 October – 1 November. <http://dx.doi.org/10.2118/162516-MS>

Shale Oil and Shale Gas Resources Are Globally Abundant. Rep. Energy Information Administration, June 2014. Web. 8 July 2014. <<http://www.eia.gov/todayinenergy/detail.cfm?id=14431>>.

Shelley, R. Saugier, L. Al – Tailji, W. et Al. 2012. Understanding hydraulic fracture stimulated horizontal Eagle Ford completions. SPE 152533. SPE/WAGE European Unconventional Resources. Vienna, Austria. <http://dx.doi.org/10.2118/152533-MS>

Sneddon, I. N. : “ The Distribution of Stress in the Neighborhood of a Crack in an Elastic Solid”, Proc., Roy. Soc. (1946) A, 187, 229.

Sondhi, N. 2011. Petrophysical characterization of Eagle Ford shale. MS Thesis, University of Oklahoma, Norman, Oklahoma, USA.

Stegent, N.A. Sorenson, F. Brake, S.C. and Fontana, C.J. 2004. Methodology to Implement the Optimum Fracture Design in an Oil-Bearing Reservoir. Paper SPE 92095 presented at the 2004 SPE International Petroleum Conference, Puebla, Mexico. 8-9, November. <http://dx.doi.org/10.2118/92095-MS>

Thompson, J. Liang P. & Mattar, L. 2012. What’s Positive about Negative Intercepts? Paper SPE 162647 presented at the Canadian Unconventional Resources Conference. Calgary, Canada. 30 October – November 2012. <http://dx.doi.org/10.2118/162647-MS>

Wattenbarger, R.A., El-Banbi, A.H., Villegas, M.E. et Al. 1998. Production Analysis of Linear Flow into Fractured Tight Gas Wells. Paper SPE 39931-MS presented at the SPE Rocky Mountain Regional/Low-Permeability Reservoirs Symposium, Denver, Colorado, USA, 5-7 April. <http://dx.doi.org/10.2118/39931-MS>

Xiang, Jiang. 2011. A PKN Hydraulic Fracture Model Study and Formation Permeability Determination. MS dissertation. Texas A&M University, College Station, Texas. December 2011.